1991

Application of resonance Raman and surface enhanced resonance Raman spectroscopies to the characterization of biomolecules: chlorophyll and hypericin

Lydia Nicole Raser
Iowa State University

Order Number 9212179

Application of resonance Raman and surface enhanced resonance Raman spectroscopies to the characterization of biomolecules: Chlorophyll and hypericin

Raser, Lydia Nicole, Ph.D.

Iowa State University, 1991

U·M·I
300 N. Zeeb Rd.
Ann Arbor, MI 48106

Application of resonance Raman and surface enhanced resonance Raman spectroscopies to the characterization of biomolecules: Chlorophyll and hypericin

by

Lydia Nicole Raser

A Dissertation Submitted to the
Graduate Faculty in Partial Fulfillment of the
Requirements for the Degree of
DOCTOR OF PHILOSOPHY

Department: Chemistry
Major: Analytical Chemistry

Approved:

Signature was redacted for privacy.

In Charge of Major Work

Signature was redacted for privacy.

For the Major Department

Signature was redacted for privacy.

For the Graduate College

Iowa State University
Ames, IA

1991

TABLE OF CONTENTS

GENERAL INTRODUCTION 1

Explanation of Dissertation Format 2

RAMAN SPECTROSCOPY 3

PHOTOSYNTHESIS 9

HYPERICIN AND PHOTOSENSITIZATION 14

SECTION I. SPECTROSCOPIC AND ELECTROCHEMICAL CHARACTERIZATION OF HALOGENATED CHLOROPHYLLS 18

INTRODUCTION 19

MATERIALS AND METHODS 23

RESULTS 27

DISCUSSION 41

Absorption Spectra 41

Electrochemistry 46

NMR 48

Resonance Raman 48

CONCLUSIONS 52

ACKNOWLEDGEMENT 52

REFERENCES 53

SECTION II. FACTORS DETERMINING STABILITY OF BACTERIOCHLOROPHYLL MONOLAYERS 57

ABSTRACT 58

INTRODUCTION 59

EXPERIMENTAL METHODS 62

Monolayers 62

HPLC and SERRS 62

RESULTS AND DISCUSSION 64

HPLC 64

SERRS 66

CONCLUSIONS 71

ACKNOWLEDGEMENT 71

REFERENCES 72

SECTION III. RESONANCE RAMAN AND SURFACE ENHANCED RESONANCE RAMAN CHARACTERIZATION OF HYPERICIN AND RELATED COMPOUNDS 73

ABSTRACT 74

INTRODUCTION 75

MATERIALS AND METHODS 80

RESULTS 82

CONCLUSIONS 99

ACKNOWLEDGEMENT 99

REFERENCES 100

SECTION IV. PHOTODYNAMIC ACTION SPECTRUM OF HYPERICIN AND LOCALIZATION OF HYPERICIN IN THE VIRUS BY SURFACE ENHANCED RESONANCE RAMAN SCATTERING SPECTROSCOPY 103

INTRODUCTION 104

MATERIALS AND METHODS 107

RESULTS 110

CONCLUSIONS 116

ACKNOWLEDGMENT 116

REFERENCES 117

GENERAL SUMMARY 119

REFERENCES 121

ACKNOWLEDGEMENT 124

To Jeff

GENERAL INTRODUCTION

Chlorophyll plays a crucial role in the conversion of light energy into usable chemical energy during photosynthesis. This process is responsible for producing the majority of our oxygenic atmosphere, many fossil fuels and raw materials. In addition to chlorophyll, many other plant pigments having important photochemical activities have been identified. One area of interest centers on those compounds which are photodynamic. These compounds may have important medical applications in the areas of cancer treatment and virus destruction. Research to understand the basic processes that drive these photochemical reactions in an effort to mimic the natural process is ongoing.

The research for this dissertation was based upon the investigation of the individual components involved in various biochemical reactions. The emphasis of this research was on the chemical and physical characterization of certain biologically important molecules. Three separate projects were undertaken. Two projects involved characterization of photosynthetic pigment derivatives while the third dealt with the spectroscopic characterization of the photodynamic biomolecule hypericin and various analogs of this compound. Several analytical techniques were used in the course of this research, particularly Raman spectroscopy.

Model compounds were utilized in each of the research projects. The use of model compounds provides a means of controlling the various parameters in more complicated systems. The use of model compounds is quite common and, within limitations, the results for model systems can be correlated to those obtained for the *in vivo* systems. However, it has been

shown that a cautious approach towards the data is warranted. Not all results obtained for the simplified model compounds are valid for the original system molecule.[1,2]

Explanation of Dissertation Format

This dissertation is arranged in an alternate format. Immediately following the General Introduction are short backgrounds on Raman spectroscopy, photosynthesis, and hypericin and photosensitization. Section I conforms to the style for publication submitted to the American Chemical Society. Section II has been accepted for publication in *Thin Solid Films.* Other authors listed on the paper are L. L. Thomas, J.–H. Kim. T. M. Cotton, and R. A. Uphaus. Section III was submitted for publication in *Photochemistry and Photobiology.* S. Kolaczkowski and T. M. Cotton are coauthors on this paper. Section IV contains preliminary results involving viral inactivation by hypericin. This work was carried out in collaboration with S. Carpenter. References cited in the General Introduction follow the General Summary.

RAMAN SPECTROSCOPY

Light interacts with molecules in several different ways. Light may be absorbed, as in uv/vis and infrared absorption spectroscopies. It may be emitted, as in fluorescence and phosphorescence spectroscopies, or it may be scattered. Raman spectroscopy measures the scattered radiation from interaction of light with a molecule. A brief review of the theory is given here. The references by Tobias[3] and Tu[4] are suggested for further reading.

Raman scattering arises if there is a change in the molecular polarizability, μ, due to a vibration. The classical equation for this process is as follows:

$$\mu = E\alpha \qquad (1)$$

If it is recognized that E, the electric field, varies with time and that α, the molecular polarizability, is dependent on the distance between the nuclei, then the equation can be expanded to its final form.

$$\begin{aligned} \mu = \quad & E_0\alpha_0\cos 2\pi\upsilon_0 t + 1/2\, E_0 Q_i^0 (\partial\alpha/\partial Q_1)_0 \\ & \times [\cos 2\pi t(\upsilon_0 + \upsilon_1) + \cos 2\pi t(\upsilon_0 - \upsilon_1)] \end{aligned} \qquad (2)$$

The first term represents Rayleigh scattered radiation, the second term Stokes Raman scattering and the third term anti-Stokes Raman scattering. Although this equation represents the three type of scattering processes, it

does not account for the difference in intensity between the different types of scattered light (illustrated in Figure 1).

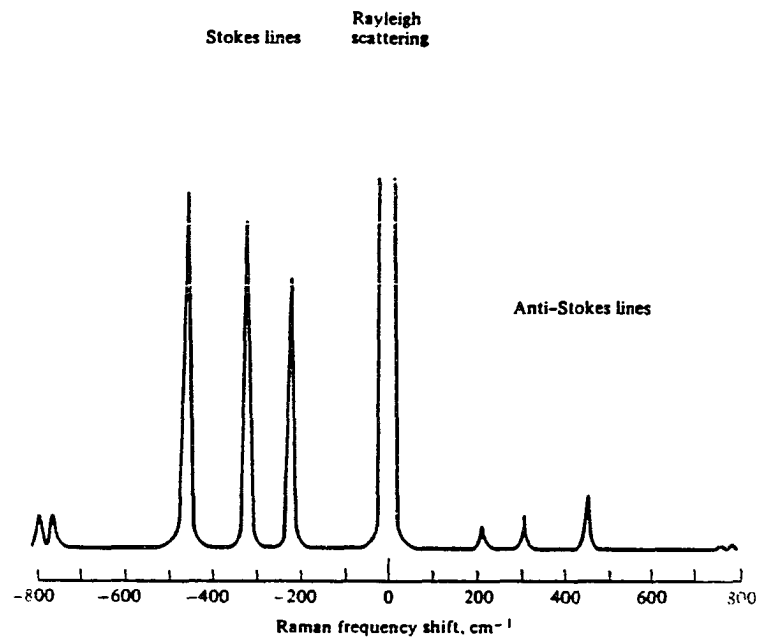

Figure 1. Relative intensities of Stokes Raman, Rayleigh, and anti-Stokes Raman lines

Energy is conserved during a collision between a photon and a molecule. The selection rules for Raman state that the change in frequency must be the addition or loss of energy associated with a molecular vibration ($\pm\Delta v$), see Figure 2. At room temperature most molecules are in the lowest vibrational level of the ground electronic state. Therefore, the molecule will be in an excited vibrational level of the ground electronic state after the photon is scattered. This corresponds to Stokes Raman scattering. A second

type of Raman scattering, called anti-Stokes Raman scattering, occurs because a small number of molecules are initially in an excited vibrational level of the ground electronic state.

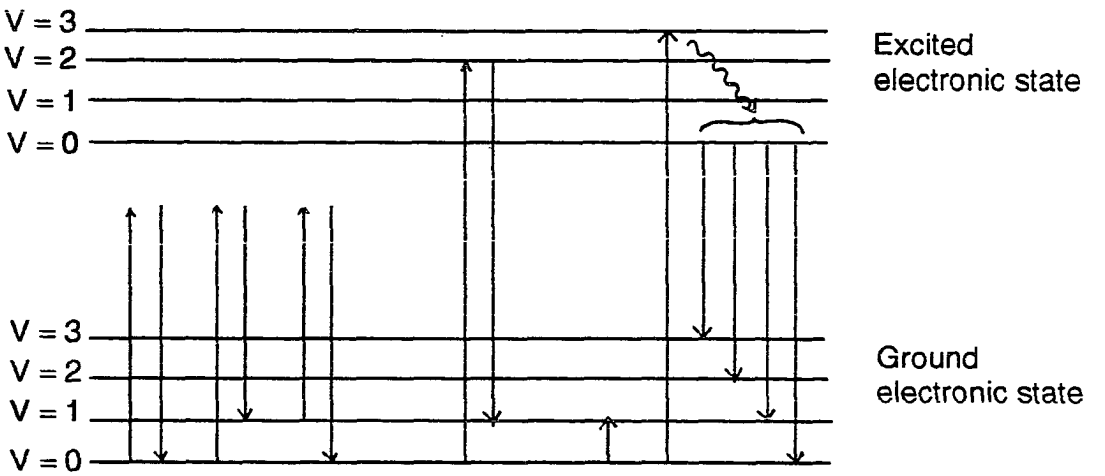

Figure 2. Origin of Raman, infrared, and fluorescence spectra. From left to right: Rayleigh scattering, Stokes Raman, anti-Stokes Raman, resonance Raman, infrared, and fluorescence

From Figure 2, it is seen that Raman and IR give vibrational information, i.e., the change in energy for both processes is equal to the difference in energy of two vibrational levels. Raman and infrared spectroscopies are complimentary techniques rather than competitive because the selection rules for the two methods are different. In infrared spectroscopy there must be a change in the dipole moment of the molecule. Therefore molecules without a dipole moment do not give an IR spectrum; for a vibrational mode to be Raman active there must be a change in the molecular polarizability. Raman has several advantages over infrared spectroscopy for

the study of biomolecules. 1) There is little interference from water in the Raman spectrum because the spectrum of water is very weak. Aqueous solutions can therefore be used and many *in vivo* systems can be studied, 2) the excitation wavelengths used for Raman are in the ultraviolet or visible region so special optics or sample holders are not necessary, and 3) small amounts of material are sufficient because the active volume is dictated by the size of the focused laser beam.

A major disadvantage of Raman spectroscopy is its inherent insensitivity (detection limits of 10^{-1} to 10^{-3} M are common). Most collisions between a photon of light and a molecules are elastic collisions, i.e., the frequency of the scattered photon is the same as the incident photon (Rayleigh scattering). On the order of one collision per one million results in a Raman scattered photon and consequently the Raman signal is very weak. In many cases, a competing process, such as fluorescence, may obscure the weak Raman signal.

The low sensitivity of normal Raman can be overcome if the excitation wavelength is chosen to coincide with an electronic absorption transition of the molecule. Under these conditions, a resonant enhancement of the vibrational modes associated with that transition occurs. This enhancement can be on the order of 10^6 fold. A resonance Raman (RR) spectrum is often simplified compared to the normal Raman spectrum as only the modes associated with the electronic transition are resonantly enhanced. Some information is lost; however, the selectivity and sensitivity of this technique compensate for this loss.

Another variation of Raman spectroscopy which was discovered in the early 1970s is surface–enhanced Raman scattering (SERS).[5-7] The surface enhanced phenomenon occurs when a molecule is adsorbed onto a roughened metal surface. The metals most often used are silver, gold, and copper although other materials may be used. From equation (1), it is seen that the magnitude of the induced dipole depends on the electric field and on the molecular polarizability; therefore, an increase in either of these terms would lead to an overall enhancement of the Raman signal. The electromagnetic enhancement mechanism states that the molecule experiences an increased electromagnetic field at the metal surface. It is known that adsorption of molecules on a metal surface affects the spectral properties of the molecule. In SERS this translates into an enhancement of the intensity proportional to the square of the electric field strength. Another consequence of the adsorption phenomenon is the quenching of fluorescence due to the energy transfer from the adsorbed molecule to the metal surface. The chemical enhancement mechanism attributes the increased signal to a large increase in the molecular polarizability that arises from adsorbate–surface interaction. It is generally agreed that both mechanisms play a role in the enhancement of the Raman signal but the relative contributions are still under discussion. The SERS effect generally increases the signal anywhere from 10^3 to 10^6 times over the normal Raman signal.

The sensitivity can be improved further if the excitation line used for SERS is coupled to an electronic transition of the molecules in RR spectroscopy. This technique is called surface–enhanced resonance Raman

scattering (SERRS) and may increase the signal by a factor of 1000 so that the overall enhancement compared to normal Raman is 10^9 to 10^{10} fold.[5-7]

PHOTOSYNTHESIS

An important aspect of photosynthesis research has been the investigation of biomimetic systems that will mimic natural photosynthesis.[8] There have been many approaches to the problem of creation of artificial photosynthetic systems. One approach has been the synthesis of molecular systems containing covalently linked chromophores, electron donors, and electron acceptors. Simple systems containing a single donor and acceptor molecule have been investigated as have more complicated systems involving three or more components.[9,10] Both naturally occurring chromophores and synthetic compounds have been utilized in these model systems. These systems must be designed so as to mimic the natural process; i.e. they must absorb light and transfer an electron from the donor molecule to the acceptor followed by formation of a "stable" charge separated state.

To understand the driving force behind this research a brief review of photosynthesis is in order. Photosynthesis is the process by which organisms convert light energy into chemical energy. There are two types of photosynthesis: 1) oxygenic – conversion of water and carbon dioxide into oxygen and carbohydrates, and 2) bacterial – this type does not have to consume water or produce oxygen. The general scheme for oxygenic photosynthesis is represented below:

$$6\,H_2O + 6\,CO_2 \xrightarrow{h\upsilon} 6\,O_2 + C_6H_{12}O_6$$

The conversion of light energy to an electrochemical gradient takes place within specially constructed membrane bound protein–pigment complexes called reaction centers (RCs). The photosynthetic pigments, chlorophylls and bacteriochlorophylls, are associated with a protein that spans a lipid bilayer. The structure and environment of the bacterial reaction center were elucidated in 1985 by Deisenhofer *et al.* [11] who were later awarded the Nobel Prize in Chemistry for their discovery.

Photosynthetic bacteria have only one reaction center (RC) which contains four bacteriochlorophylls (Bchl *a*), 2 bacteriopheophytins (BPheo *a*), two quinones, and a nonheme iron. These components are arranged in an approximate C_2 symmetry (Figure 3); however, the electron transfer occurs down only one side of the two branches. Considerable debate has been generated as to why only one branch is active.[12,13] The primary electron donor is a specialized Bchl *a* pair (SP). Light energy is absorbed by accessory (antenna) chlorophylls, called light harvesting chlorophylls (LHC), and is funnelled to the photosynthetic reaction center where the primary charge separation occurs. The special pair is electronically excited to its lowest singlet excited state by excitonic energy transfer from the antenna molecules. The electron from the special pair is then transferred to the BPheo *a* and then on to the first quinone and then to the second quinone. A second electron is then transferred down the pathway. The net result of this electron transfer is the generation of a charge separated state across the lipid bilayer. The forward process is extremely fast, with essentially a quantum efficiency of one, while the back reaction is minimal. This primary charge separation is subsequently coupled to the formation of energy rich molecules.[14]

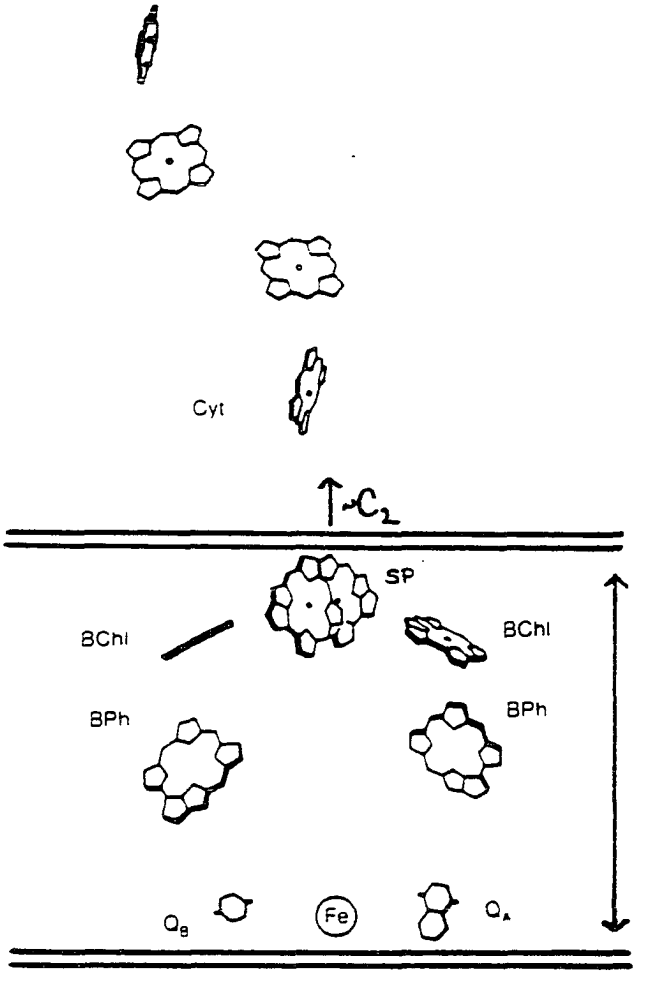

Figure 3. Arrangement of photosynthetic pigments in the bacterial reaction center. From Gregory [14] and based on the structure published by Deisenhofer *et al.* [11]

In contrast to photosynthetic bacteria, higher plants contain two distinct reaction centers, Photosystem I (PS I) and Photosystem II (PS II). The fundamental aspects of these reaction centers have been reviewed.[41] The two photosystems work in tandem; PS I oxidizes plastiquinone and reduces NADP while PS II oxidizes water and reduces plastiquinone. The second phase of photosynthesis is the conversion of CO_2 into carbohydrate. This takes place during the dark cycle (Calvin cycle).

PS II in higher plants has many similarities to the bacterial reaction center. The primary donor (P680) is most likely a Chl a dimer in a specialized environment. There are also similarities in the protein subunits surrounding the RC pigments and the RC photochemistry parallels events that occur in the PS of purple bacteria.[15-18]

Much less in known about the structure of PS I because there is no equivalent structure in the bacterial systems. However, it is thought that the primary donor (P700) is a Chl a dimer bound to the protein although Chl derivatives have not been ruled out.[19]

Our interests are focused on the primary events in photosynthesis, i.e., electron transfer in the reaction centers. To enhance our understanding model systems are utilized; however, many problems may be encountered while working with model systems. As mentioned above, these systems may include either natural or synthetic components. If natural pigments are used, degradation products may be readily formed. These natural constituents are very stable in their natural membrane systems but they are more easily degraded *in vitro*. Knowledge of expected degradation products and the

conditions which minimize their formation is needed to maintain the integrity of the biomimetic membrane systems.

HYPERICIN AND PHOTOSENSITIZATION

Hypericin is a photodynamic quinoidal compound found in certain species of the genus Hypericum. Hypericin has been found to exhibit a variety of photodynamic effects.[20] Hypericism, a condition of severe sensitivity to sunlight was observed to occur in animals, especially those animals with white fur or light skin, after ingestion of this species of plants.[21,22] Early experiments had shown that photosensitization required both light and oxygen.[23] Hypericin photosensitization was therefore classified as belonging to the category called photodynamic action. The definition of photodynamic action used here is that of Blum:[24] "The sensitization of a biological system to light by a substance which serves as a light absorber for photochemical reactions in which molecular oxygen takes part." These photooxidations are quite different than those occurring during normal cellular metabolism. There are, however, other types of sensitization requiring light that do not fall under this definition but these will not be discussed here.

In addition to inducing photosensitivity, it was discovered that hypericin is the chromophore of the *Stentor* photoreceptor (stentorin) that is responsible for the negative phototactic response of the ciliates.[25-27] It is also known to have bactericidal properties and was used at one time as an antidepressant.[28] Recent findings have also determined that hypericin shows a photodynamic effect against several retroviruses, including HIV.[29-33]

Hypericin has been shown to form radical anions, a Type I mechanism, and to produce singlet oxygen, a Type II mechanism, in *in vitro* experiments.[34-37] Figure 4 shows the two different processes. Based on

studies involving structurally similar compounds it is thought that hypericin most likely induces its photodynamic effects through the production of singlet oxygen although the role for a radical mechanism cannot be ruled out.[35,37]

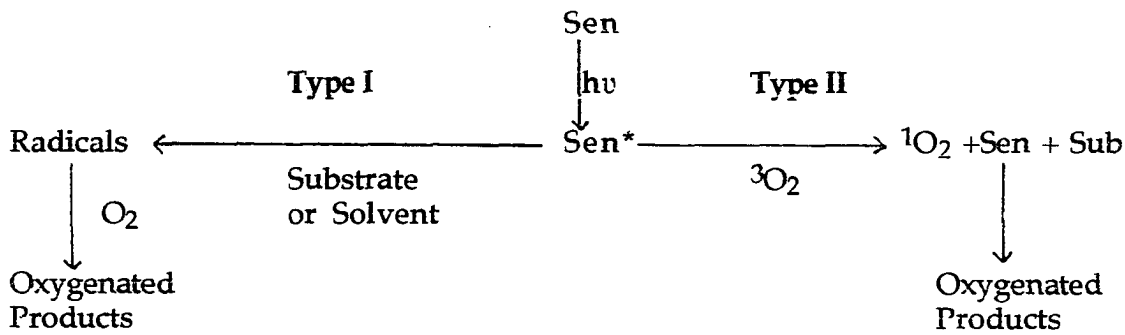

Figure 4. Mechanisms of photosensitized oxidation. From Foote[11]

Type I Electrons are more easily transferred in the excited state than from the ground state. This type of mechanism is the result of an electron being promoted from a strongly binding orbital to one that is less strongly binding when going from the ground to excited state. The radical anion of the sensitizer is immediately reoxidized by oxygen to give a superoxide–ion radical cation pair. Hydrogen abstraction may also occur to give radical products. These may then react with oxygen to give peroxides and initiate radical chain autooxidation.[36]

Type II This mechanism involves the formation of an excited state of the sensitizer which then reacts with triplet oxygen ($^3O_2$) to produce

singlet molecular oxygen ($^1O_2$). The $^1O_2$ reacts with the substrate to give oxygenated compounds.[38]

Several methods may be utilized to distinguish between these two mechanisms. The lifetime of singlet oxygen depends on the solvent; therefore, a Type II process can be distinguished from a Type I mechanism by changing the solvent, e.g., deuterating the solvent and monitoring the singlet oxygen lifetime. If the photodamage is caused by a radical mechanism, then deuterating the solvent should have no effect on the amount of oxygenated products. In addition, singlet oxygen quenchers can be added to the reaction mixtures. These will obviously compete with the substrate for the oxygen which results in a decrease of the expected oxygenated products. For a radical mechanism, the sensitizer and substrate must be in close contact at the time of reaction, whereas $^1O_2$ is known to be mobile and is capable of migrating through biological membranes and aqueous phases.[39,40]

The objective of this research is to correlate the structure of hypericin with its biological activity. The approach is to use RR and SERRS spectroscopies together with suitable model compounds and correlate the spectroscopic properties with hypericin's activity. Preliminary work with *in vitro* viruses containing hypericin has elucidated the SERRS spectrum of hypericin in the presence and absence of virus. This aspect of the project has two objectives: 1) as there are many different sites where photodamage by hypericin may occur, the location of the hypericin within the virus must be determined and 2) the mode of action of hypericin needs to be identified as either a Type I or a Type II mechanism or a combination of both. With respect to these objectives, binding of sensitizer to substrate has been shown

to favor a Type I mechanism. Type II mechanisms are more probable if the sensitizer and substrate are physically separated. Several interactions between sensitizer and membranes have been observed. 1) No interaction - i.e., $^1O_2$ is generated external to the membrane followed by diffusion of the $^1O_2$ to the membrane. This has not been found to be a common occurrence in biological systems. 2) Sensitizer bound to the membrane. This encompasses two types of binding: a) sensitizer is attached to the membrane though a ligand or b) sensitizer is incorporated into the membrane.[40]

Both objectives may be reached by utilizing model membrane systems incorporating hypericin. The effect of location and environment on the spectroscopic properties of hypericin can be examined and various techniques will be used to elucidate the mechanism for photodynamic action.

SECTION I. SPECTROSCOPIC AND ELECTROCHEMICAL CHARACTERIZATION OF HALOGENATED CHLOROPHYLLS

INTRODUCTION

The driving force behind much of the recent photosynthesis research has been the desire to create an artificial system that mimics the conversion of light into chemical energy that takes place during photosynthesis. This type of research has been approached from many different angles.[1] The exact structure and arrangement of the photosynthetic pigments in the reaction centers of green plants is still unknown, although a general consensus has been reached. Several structures have been proposed for the primary donors of Photosystem I and Photosystem II including chemically modified Chl *a* [2] and Chl *a* dimers. Based on comparison with reaction centers from purple bacteria, it is thought that the primary donor in PS II is a Chl *a* dimer. However, the PS I reaction center is more difficult to determine because of the lack of a corresponding system in the purple bacteria.

In the early 1980s, chlorinated chlorophylls and related compounds generated considerable interest because these compounds were thought to be natural components of photosynthetic plants.[3] It was proposed that a chlorinated and hydroxylated chlorophyll a (13^2–OH–20–Cl–Chl *a*) was an integral part of the reaction center (RC) of Photosystem I (PS I) in higher plants and cyanobacteria.[4] RC I was found in a 1:1 ratio with P700, the chlorophyll protein complex identified as the reaction center, and was thought to be the reaction center chlorophyll. A series of papers were published detailing the structure, function and biosynthesis of Chl RC I.[5,6] However, later studies proved this compound to be a preparation artifact formed during TLC purification of the reaction center pigments.[7] Details of its synthetic formation and subsequent purification were later published.[8-11]

Although no longer of interest as an integral part of the RC, halogenated chlorophylls, pheophytins and decarbomethoxylated derivatives deserve further attention. Addition of a halogen to the chlorin macrocycle induces changes in both chemical and physical properties [12-17] which make these compounds interesting. In addition, because the halogen is a better leaving group than the hydrogen atom, the halogenated compounds may be used as intermediates in the synthesis of models for photosynthetic components.

In 1964 Woodward and Skaric [18] demonstrated that chlorins, with one reduced ring, are susceptible to electrophilic attack at the meso carbons adjacent to the reduced ring. This susceptibility is due to an increased electron density at the methine positions next to the pyrrole ring. Porphyrins without the reduced ring did not undergo electrophilic substitution at the meso positions. However, several papers have since been published documenting meso substitution, including halogenation, of porphyrins.[19-21] In Chl *a* and related compounds (Figure 1) the γ meso carbon is blocked and only the δ position remains accessible. It is thought that bacteriochlorophylls (BChl's) with two reduced rings should readily undergo electrophilic attack at more than one meso position. However, this reaction has not been attempted yet.

The objectives of this research were as follows: 1) Synthesis of specifically modified chlorins with electrophilic substitution of halogens at the C–20, delta meso, position. 2) Correlation of the electronic and steric effects of the halogen substitution with the spectral and electrochemical properties of

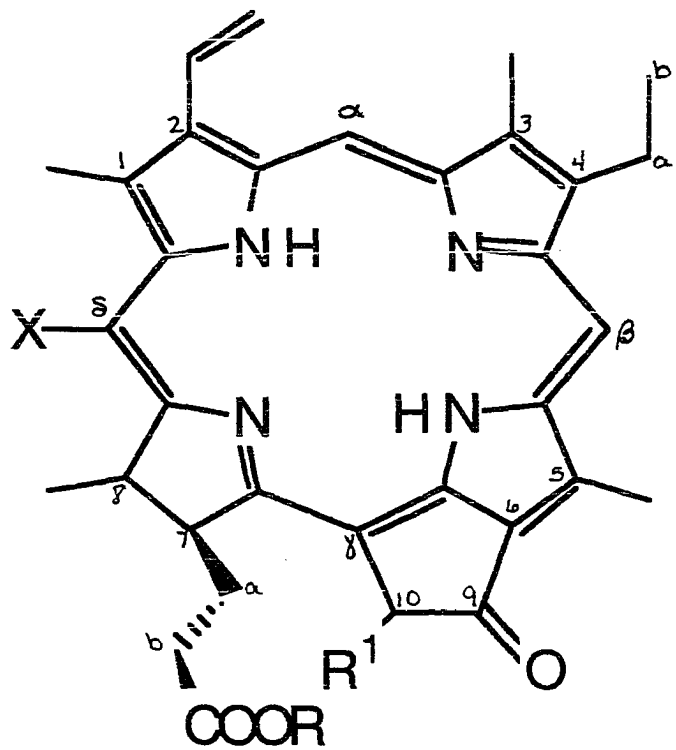

Compound	R	R^1	X
MPP *a*	CH_3	H	H, F, Cl, Br
Pheo *a*	$C_{20}H_{39}$	$COOCH_3$	H, Cl, Br
PPheo *a*	$C_{20}H_{39}$	H	H, Cl, Br

Figure 1. Structures of Methylpyropheophorbide *a*, Pheophytin *a*, Pyropheophytin *a*, and halogenated derivatives

chlorins. 3) Use of the halogenated chlorophylls as intermediates in the synthesis of model compounds formed in transformation of the C–20 position. Products of the coupling reactions would be dyads or triads to be used to investigate electron transfer properties.

The first two goals have been met and some preliminary work on the third objective was begun. The majority of the work presented here deals with MPP *a* and its halogenated derivatives (X–MPP *a*, where X = H, F, Cl, and Br). Unless otherwise noted, the results presented here will be for these compounds. Any differences observed between the three halogenated series will, of course, be discussed. However, the conclusions drawn for X–MPP a should be valid for the other compounds as well.

MATERIALS AND METHODS

Total plant pigments were extracted from spinach following the procedure established by Strain and Svec.[22] Chl *a* was separated from the total pigment extract by reverse phase high performance liquid chromatography (rp HPLC). Pheophytin *a* (Pheo *a*) was synthesized from Chl *a* by dissolution in diethyl ether followed by acidification with HCL. PyroChlorophyll *a* (PChl *a*) was prepared by refluxing (150 C) Chl *a* in 2,4,6–collidene for approximately 2 hours.[23] The solvent was removed under vacuum and the crude product purified by rp HPLC. PPheo *a* was obtained using the same method as for Pheo *a*. These compounds were purified using a preparative scale Spherisorb ODS 10 mm column (22.5 mm x 25 cm) with a flow rate of 8 ml/min. To preserve the column packing, a guard column filled with C_{18} packing was placed in front of the main column. The major portion of the Chl *a* peak was collected. An isocratic mobile phase system of acetone/ethanol/doubly deionized water (55:30:15) was used. The solvents were vacuum filtered (0.45 μm filter) and degassed prior to use. To check the purity of sample collected from the preparative column, a Phenomenex Ultrex 3 mm 4.6 mm x 7.5 cm column with flow rate of 1 ml/min was used. Detection for both systems was accomplished by use of a uv/vis detector set at 445 nm.

Methyl pyropheophorbide *a* (MPP *a*) was synthesized by dissolving PPheo *a* in 5% sulfuric acid in methanol and stirring overnight in a nitrogen atmosphere. The crude product was diluted with methylene chloride and neutralized with ammonium bicarbonate. The organic phase was collected and the solvent evaporated.[23] Purified MPP *a* was isolated on an ISCO

Spherisorb Si 5 mm 10 mm x 25 cm column with a flow rate of 1 ml/min (methylene chloride/ethyl acetate, 95:5; λ_{det} = 425 nm).

The method published by Scheer *et al.*[6] was used with minor modifications for the chlorination (or bromination) reactions for all compounds except for Chl *a*. To the pigment solution in diethyl ether, (approx. 1 mg/7 ml) an equal volume of acid (16% hydrochloric acid or 5% hydrobromic acid) was added under gentle stirring. Next, 30% hydrogen peroxide (1 mg pigment/8 ul H_2O_2) was added to the reaction mixture. The flask was stoppered to prevent loss of solvent during the reaction. The reaction was deemed complete after a color change was observed (30 minutes for chlorination, 15–20 minutes for bromination). Progress of the reaction was monitored by absorption spectroscopy and analytical HPLC. When completed, the reaction mixture was diluted with ether and washed until neutral with a 10% sodium bicarbonate solution. The ether phase was collected and the solvent evaporated under reduced pressure. Crude mixtures were purified using the same HPLC conditions listed above for the parent compound.

The fluorinated derivative of MPP *a* was provided by T. Michalski of Argonne National Laboratory. The method of synthesis is published elsewhere.[24]

For RR experiments, the purified pigments were dissolved in anhydrous ether (or HPLC grade methylene chloride) and placed in 5 mm o.d. Pyrex tubes, vacuum degassed using three freeze–pump–thaw cycles and sealed under vacuum. Samples were then stored at 0 C in the dark.

The RR spectra were obtained with laser excitation lines as follows: Coherent Innova 100 Kr^+ (406.7 nm) or Coherent Innova 90 Ar^+ (514.5 nm) lasers. The laser power was approximately 25 mW at the sample; total integration time was 170 seconds. Raman scattered radiation was collected in a backscattering geometry. Resonance Raman spectra were recorded on a multichannel system consisting of a Spex Triplemate 1877 spectrometer, containing an 1800 groove/mm grating in the spectrograph stage, a water cooled PARC 1420 diode array detector and a PARC OMA II multichannel analyzer. Indene was used for frequency calibration. All spectra were recorded at room temperature.

$E_{1/2}$ values for the first one electron oxidation-reduction cycle were determined for MPP *a* and its halogenated derivatives in the following manner. A millimolar solution of MPP *a*, or derivative, was dissolved in methylene chloride (CH_2Cl_2) containing 0.1 M tetrabutylammonium-perchlorate (TBAP) and ferrocene. This solution was then placed in a specially constructed vacuum spectroelectrochemical cell and degassed by three freeze-pump-thaw cycles. A silver chloride coated silver wire was used as a quasi-reference electrode to avoid introducing water into the sample solution, as would happen with an aqueous reference electrode. The potential shifts of the halogenated compounds were measured relative to the ferrocene/ferricinium redox couple. The half-wave potential of the ferrocene/ferricinium couple was then measured against a saturated calomel electrode (SCE) reference electrode under the same experimental conditions. The measured values therefore contain a constant junction potential.

The structures of the synthesized compounds were verified by absorption spectroscopy as well as ^{1}H NMR. The series of X–MPP *a* was also further identified by plasma desorption mass spectrometry (PDMS). The PDMS spectra were acquired by Dr. J. Hunt at Argonne National Laboratory.

RESULTS

Halogenation was observed to occur from the color change of the reaction mixture. For MPP *a*, the compound most studied, the initial solution was greenish brown. As halogenation occurred, the solution became a plum color. If the reaction was quenched shortly after the onset of the plum color, the major reaction product was the desired halogenated compound with the remainder being unreacted starting material. If the reaction was allowed to proceed for a longer period of time, the yield, approximated by HPLC peak area, for the 20–halogenated compound decreased and other products were formed. These products were most likely halogenated as well but we were unable to obtain them in sufficient quantities for NMR spectroscopy. Previous studies involving porphyrins have shown that the site of halogenation was affected by both the size and reactivity of the halogen involved.[21-25] Halogenation at the meso position was favored if the halogen was small and reactive, e.g., chlorine. For the larger and less reactive halogens, bromine (and iodine), if competition for substitution at the beta carbons or the meso position was possible, halogenation at the beta positions was favored. Bromination did occur at the meso position if excess bromine was used. The reason for these results was attributed to lack of steric interference at the beta carbons of the macrocycle. In such cases halogenation is more likely to occur at a less sterically hindered location i.e. the beta carbons of the macrocycle.[25]

The absorption spectra of the halogenated compounds are shown in Figure 2. The major absorption bands are identified in Table 1 as are the bands for the other compounds studied here. Halogenation appears to affect

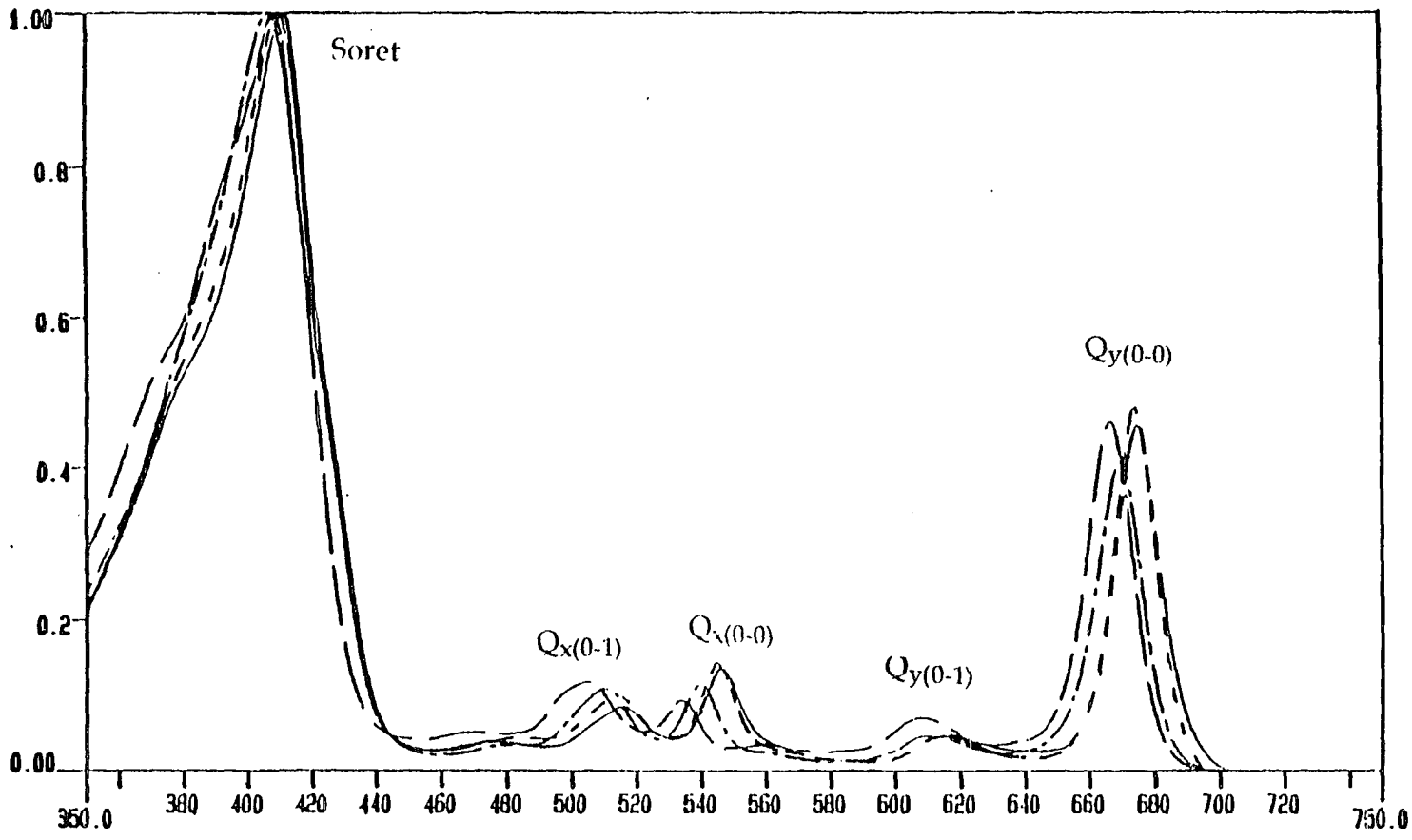

Figure 2. Absorption spectra of MPP a (——), F-MPP a (——), Cl-MPP a (——), and Br-MPPa (——) in ether

Table 1. Absorption bands of halogenated compounds

Compound	Soret[a,b]	$Q_{x(0-1)}$	$Q_{x(0-0)}$	$Q_{y(0-1)}$	$Q_{y(0-0)}$
H-MPP *a*	408	505	535	608	666
F-MPP *a*	407	511	540	612	670
Cl-MPP *a*	410	515	545	616	674
Br-Mpp *a*	411	515	546	618	675
H-Pheo *a*	408	504	532	610	668
Cl-Pheo *a*	408	514	544	618	676
Br-Pheo *a*	410	514	546	618	676
H-PPheo *a*	408	506	534	610	668
Cl-PPheo *a*	410	514	546	618	674
Br-PPheo *a*	410	516	546	618	676

[a] Electronic transition (from Figure 2).
[b] Wavelengths are in nanometers (nm).

primarily the Q transitions, as these are the bands that experienced the most change upon derivitization, as evidenced by wavelength shifts to the red and changes in relative intensities between bands. However, the Soret band also showed minor shifts upon halogenation although the shifts were not consistent, i.e. the Soret band for the fluorinated derivative showed a 2 nm blue shift whereas the chlorinated and brominated compounds showed red shifts of 2 and 3 nm respectively. The overall similarity of the absorption spectra suggests that the π–system is not greatly perturbed by halogen substitution.

On a reverse phase HPLC column with the mobile phase used, the halogenated compounds were eluted at longer retention times than the parent compound. The order of elution by substituent at the C–20 position was H–, Cl– and then Br–. As expected, this order was reversed when the normal phase column was used for separation. Table 2 lists the retention times for MPP *a* and derivatives. Retention times for the fluorinated and chlorinated derivatives of MPP *a* were quite similar (less than 30 sec difference) under the original conditions. Lack of sufficient amounts of the fluorinated derivative limited the development of a separation procedure.

Table 2. HPLC retention times (in minutes) for MPP a and derivatives

H-MPP a	17.6
F-MPP a	11.6
Cl-MPP a	11.9
Br-MPP a	10.8

Table 3. NMR chemical shifts (in ppm) and assignments.

MPP *a*	Br-MPP *a*	Assignment[a]
9.5	9.5	β
9.3	9.4	α
8.3		δ
8.0	7.8	=CH (2)
6.3	6.2	H-trans (2)
6.2	6.0	H-cis (2)
5.2	5.1	H-C_{10}
4.4	4.7	H (8)
4.2	4.1	H (7)
3.7	3.6	-$COOCH_3$ (7)
3.6	3.4	-CH_3 (5)
3.4	3.5	-CH_3 (1)
3.2	3.2	-CH_3 (3)
2.4	2.4	H (7a and a')
2.3	2.1	H (7b and b')
1.8	1.5	-CH_3 (8)
1.7	1.6	-CH_3 (4b)

[a] Assignments are from Katz *et al.* [40]

1H NMR spectra were measured to determine structure. The proton chemical shifts and assignments for MPP *a* and its brominated derivative are listed in Table 3. The parent compounds and the halogenated derivatives were readily distinguished by the disappearance of the delta methine proton in the derivatives. In addition, several shifts in the proton resonance frequencies of the halogenated compounds were noted. The proton assigned to H at position (8) is shifted upfield while the methyl protons at position (1) are shifted downfield as are the protons on the methyl group at position (8). In chlorinated porphyrins, the b protons adjacent to the meso-chloro atom was reported to be shifted downfield by approximately 0.4 ppm.[25]

PDMS spectra (not shown) of the halogenated MPP *a* compounds were determined. The spectra identified the parent ion of the halogenated compounds as being 18, 34 or 36, or 78 or 80 mass units higher than the hydrogen substituted MPP *a*. There was no indication of di–halogenation occurring.

Half-wave potentials for the halogenated MPP *a* series were measured and the average values are listed in Table 4. The $E_{1/2}$ values became more positive with the C–20 substituent according to the following order: H < F < Cl < Br.

Table 4. Half-wave potentials vs. SCE for first one electron oxidation of MPP *a* and halogenated derivatives

Compound	Oxidation Potential
H-MPP *a*	+863 ± 6 mV
F-MPP *a*	+916 ± 8 mV
Cl-MPP *a*	+938 ± 13 mV
Br-MPP *a*	+940 ± 11 mV

The RR spectra in Figs. 3, 4, and 5, were obtained with laser excitation into the Soret band at 406.7 nm. The Soret is an intense transition for all compounds and does not experience a large shift in wavelength on halogenation. Because of this, large changes in the RR spectra are not expected. In all cases, the chromophore, i.e. the macrocycle, is the same and only a small change in structure has been made. The chromophore is resonantly enhanced at 406.7 nm and the same vibrations are enhanced in all spectra at this wavelength. However, frequency changes for vibrational modes associated with the halogen substitution would be expected; and there are several frequency changes that are attributable to the halogen substitution. Table 5 lists the major Raman bands and their assignments for the compounds studied. The assignments were taken from several references and are based on both theoretical and experimental results.[26-28, 30, 39] The high frequency region (1000 – 1750 cm^{-1}) is composed of in–plane stretching and bending modes while the low frequency region (200 – 1000 cm^{-1}) is characterized by in–and out–of–plane bending vibrations.

The bands most affected in all spectra, with 406.7 nm excitation, are the following: the 1624 cm^{-1} band appears to downshift, the 1607 cm^{-1} band increases in intensity with halogenation, the shoulder at 1555 cm^{-1} separates from the major peak at 1580 cm^{-1} and grows in intensity, the 1535 cm^{-1} band downshifts to 1513 cm^{-1} and the intensity increases, the band at approximately 1495 cm^{-1} is upshifted and increases in intensity, the bands at approximately 1030 cm^{-1} also shift up in frequency, the band at approx. 895 cm^{-1} decreases in intensity and downshifts slightly, and two bands at 790 and

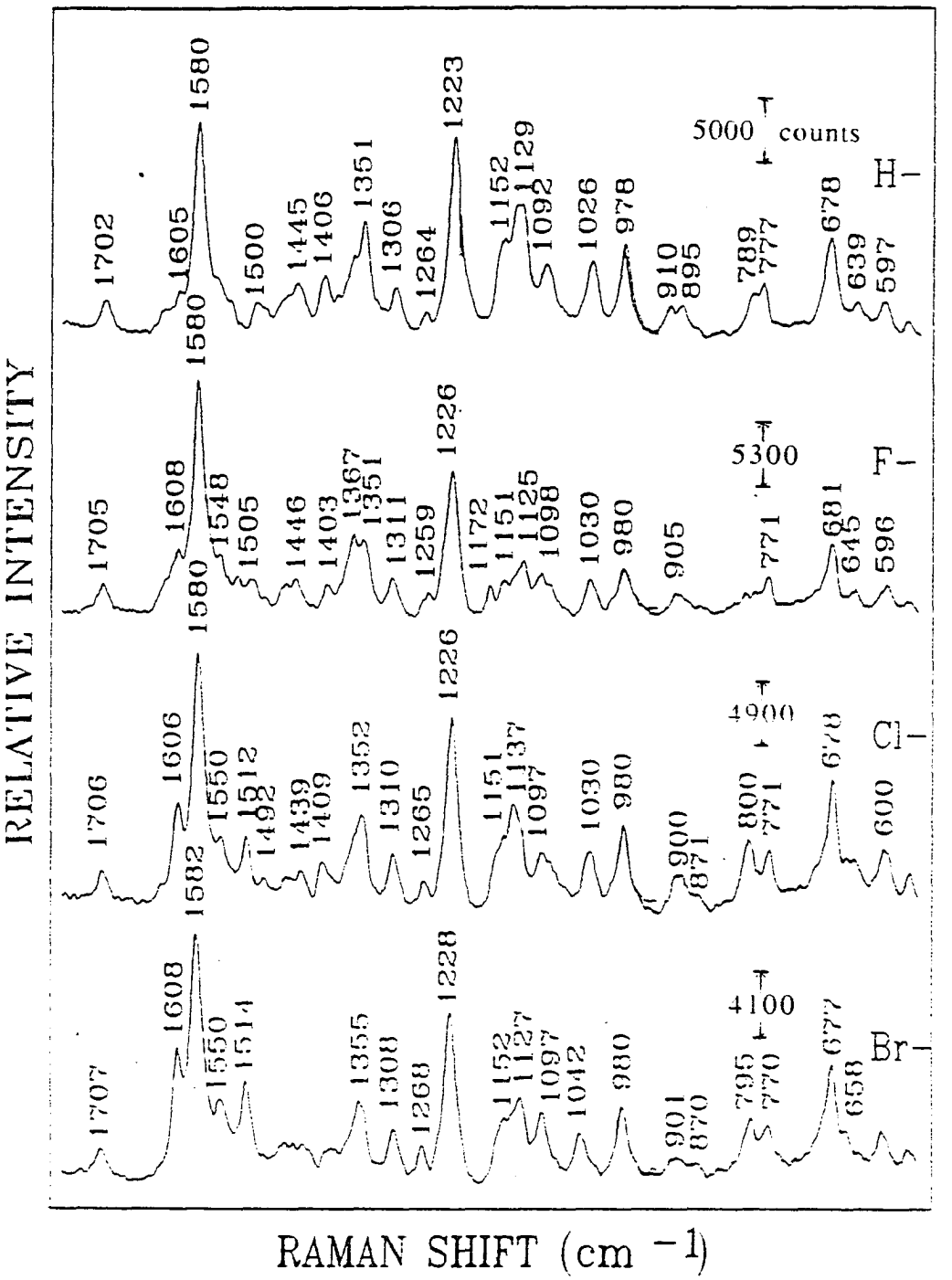

Figure 3. Resonance Raman spectra of MPP *a* in ether, λ_{ex} = 406.7 nm.

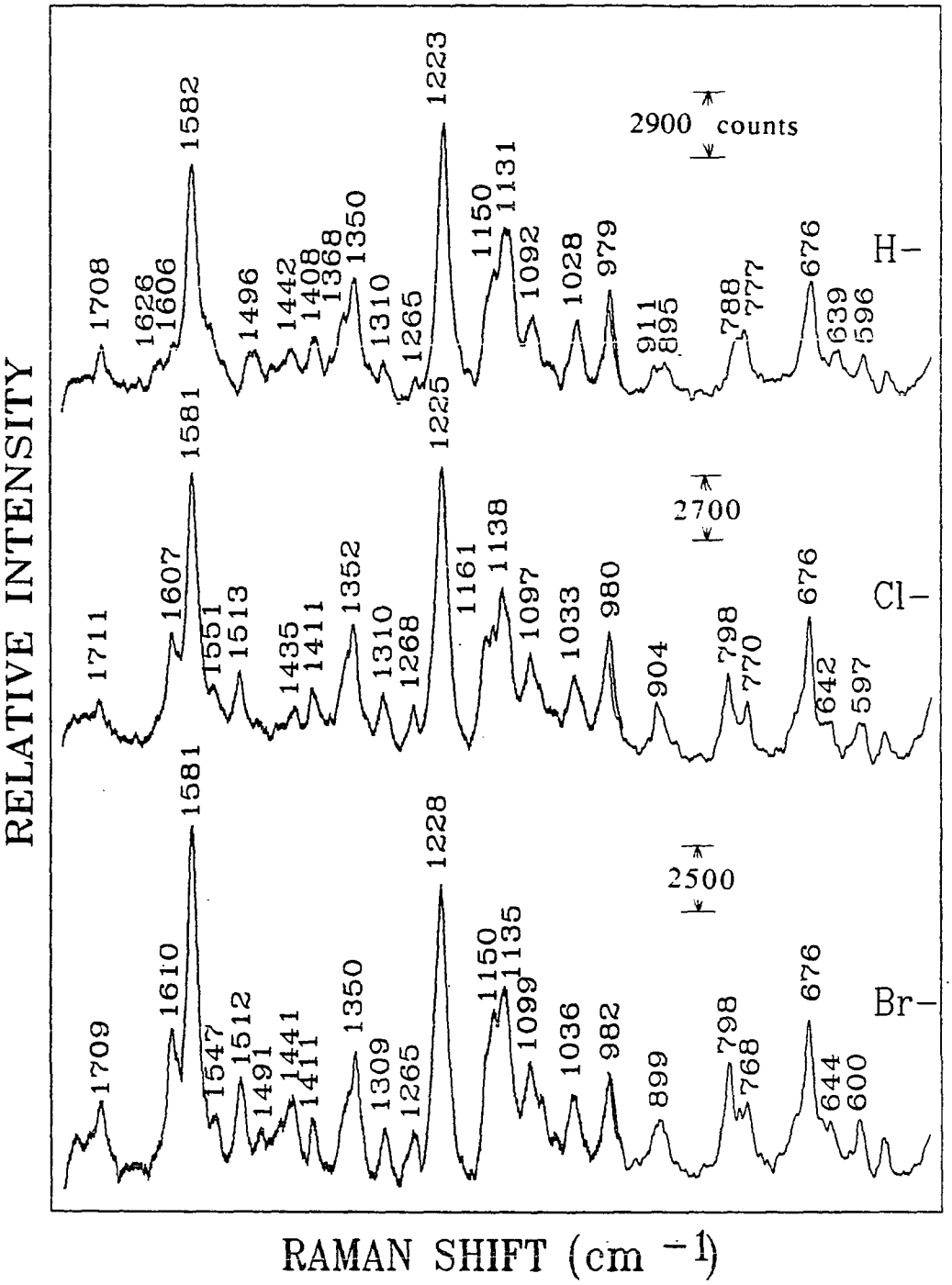

Figure 4. Resonance Raman spectra of PPheo *a* in ether, λ_{ex} = 406.7 nm

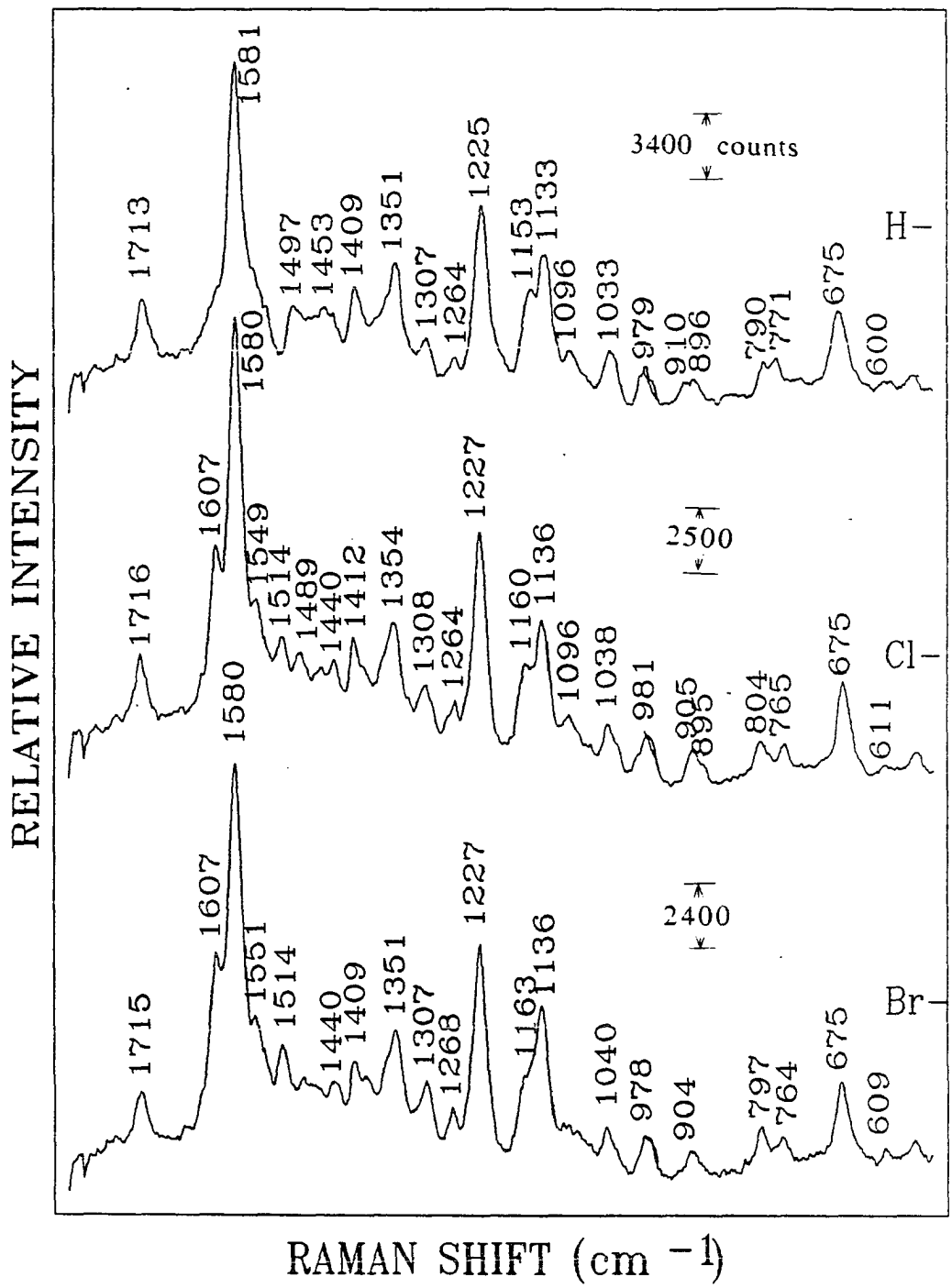

Figure 5. Resonance Raman spectra of Pheo *a* in ether, λ_{ex} = 406.7 nm

775 cm^{-1} shift apart and the higher frequency band becomes more intense. These changes were seen in all spectra.

514.5 nm excitation (Figures 6, 7, and 8) was used to probe a different electronic transition. In the halogenated compounds the $Q_{x(0-1)}$ absorption band is shifted from 505 nm to 516 nm which should result in a larger resonant enhancement of the halogenated compounds compared to the unsubstituted compounds. Unfortunately, the extinction coefficient at this wavelength is very low compared to the Soret transition and the resonant enhancement is therefore small. Also, at this wavelength, fluorescence is stronger. It was thought that substitution by a halogen would quench fluorescence. This did occur for the bromo substituted MPP *a* but was not observed in the spectra of the other derivatives. In addition, the overall quality of the spectra were not good.

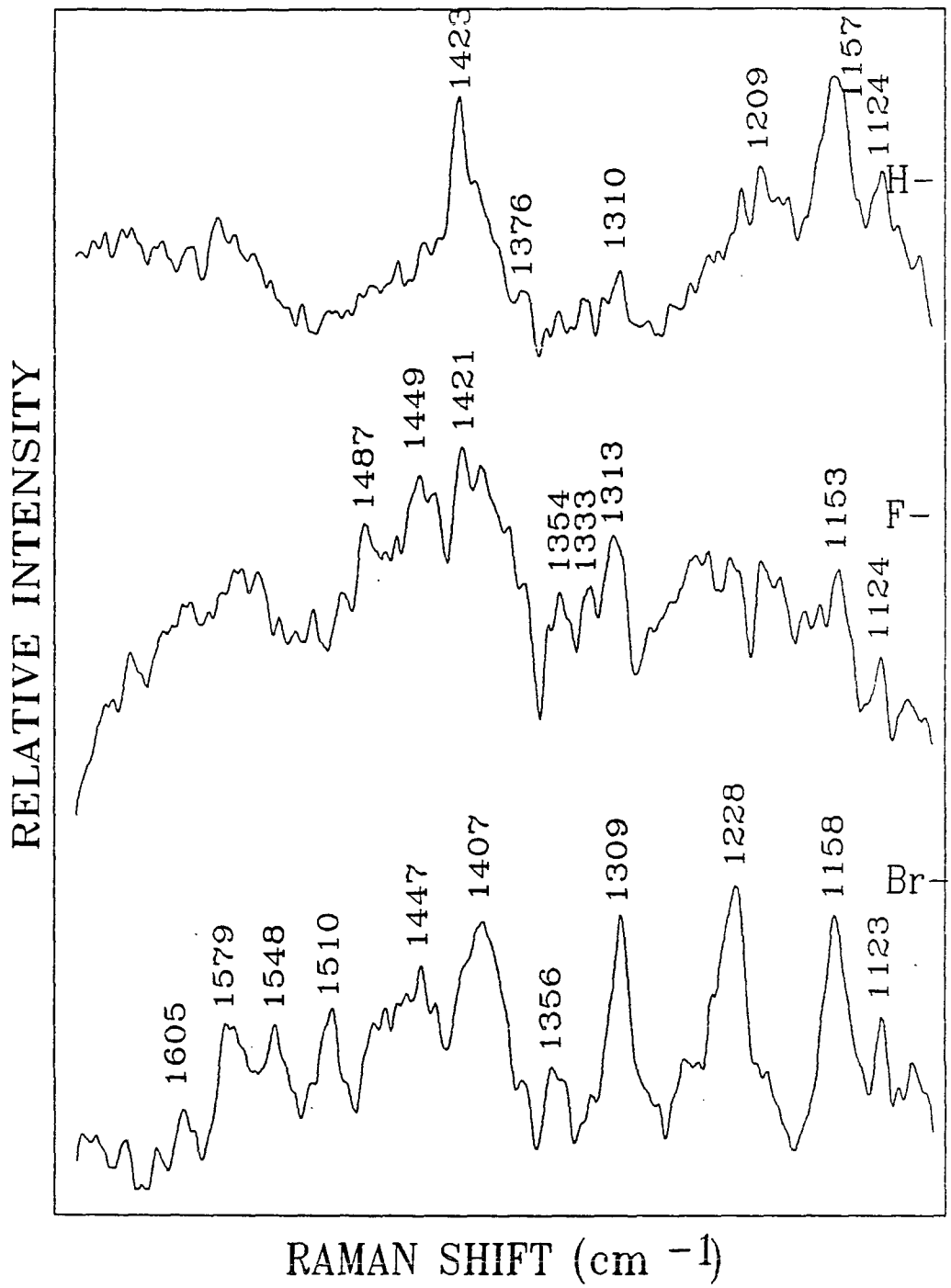

Figure 6. Resonance Raman of MPP *a* in CH_2Cl_2, λ_{ex} = 514.5 nm

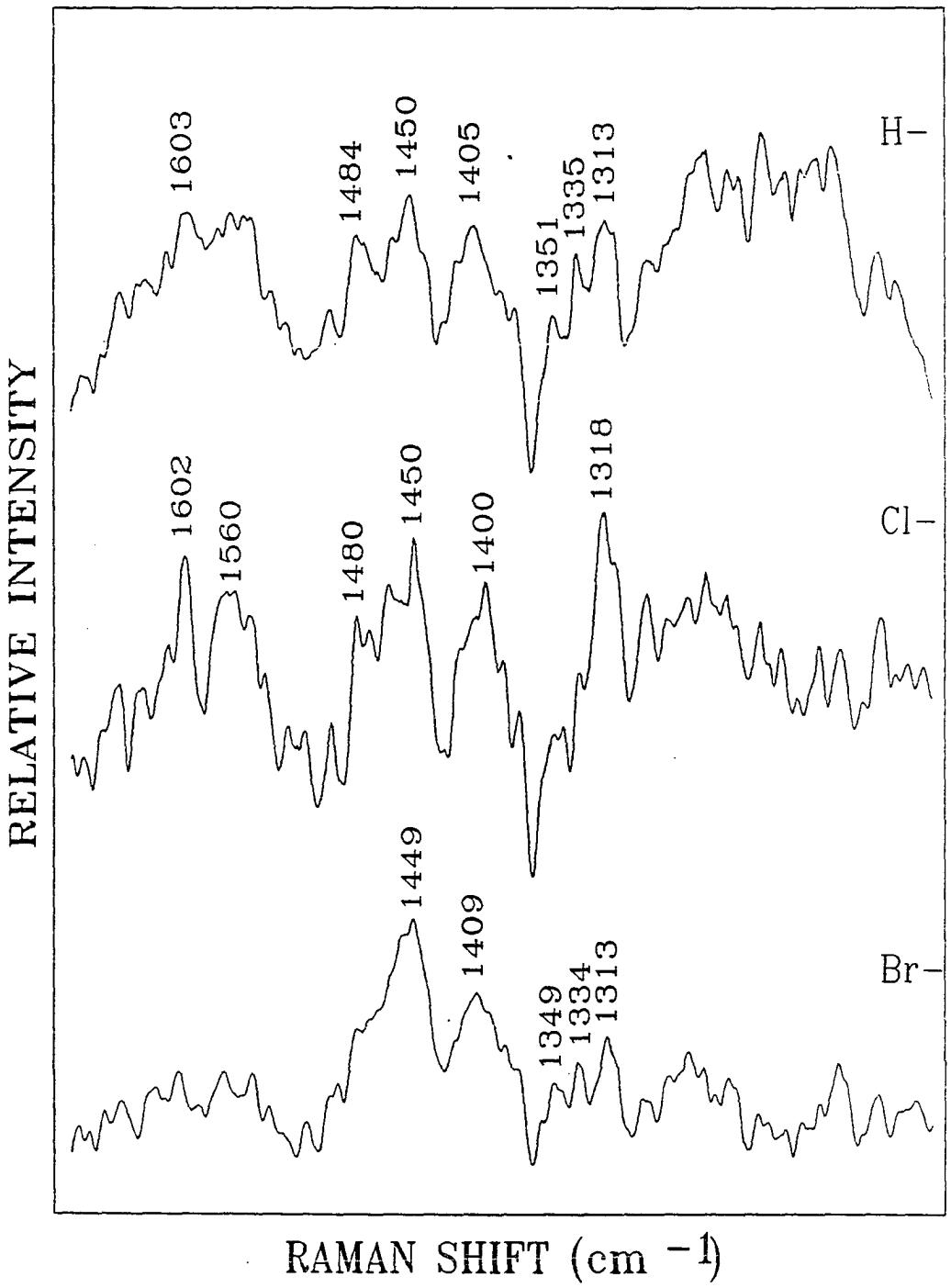

Figure 7. Resonance Raman of PPheo *a* in ether, λ_{ex} = 514.5 nm

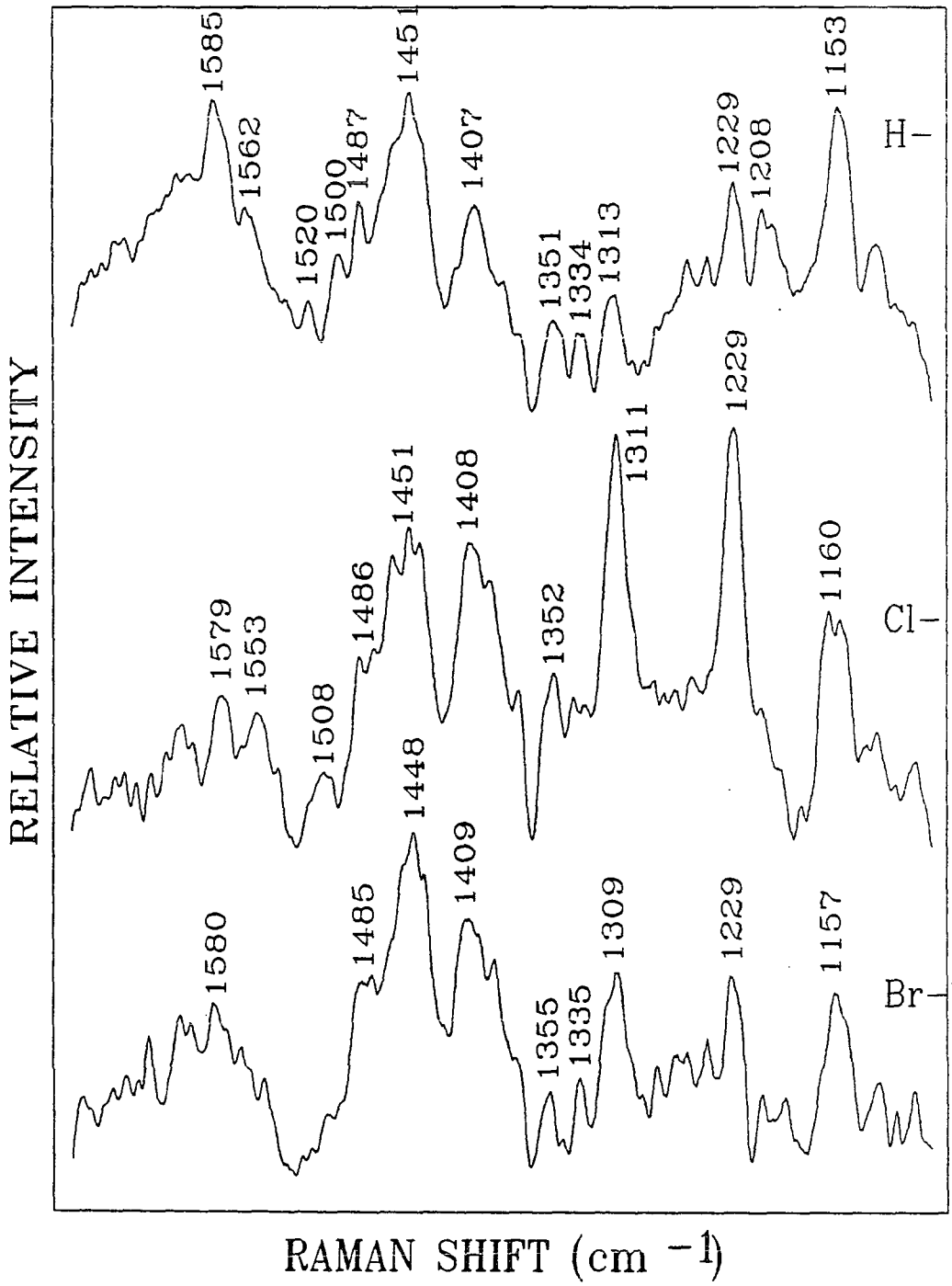

Figure 8. Resonance Raman of Pheo *a* in ether, λ_{ex} = 514.5 nm

DISCUSSION

Halogens are electron withdrawing groups, considerably larger in size than hydrogen, and addition of such a group to the chlorin macrocycle will affect the physical and chemical properties. With the addition of the halogen the electron density of the macrocycle is decreased simply because of the electron withdrawing nature of the halogen as compared to the hydrogen atom that was replaced. An effect due solely to the electronegativity of the halogen is expected to be greatest for the fluorinated derivative. This effect could be ascribed to either inductive or resonance effects or a combination of both. In addition, there may also be a steric effect due to the size of the halogen, which would be more pronounced with the larger halogens, i.e. bromine.

The literature contains many examples of experiments in which the effect of various substituents on the spectral and electrochemical properties of porphyrins were studied.[12-17,31-34] These experiments, however, concentrated on porphyrins, not chlorins, and the substitutions were symmetric. This work reports the effect of a single substitution on the chlorin macrocycle; however, many of the conclusions drawn in the previous work can be applied to the systems studied here.

Absorption Spectra

The changes that occur in the absorption spectra with halogen substitution may be explained to a limited extent by the four orbital model for porphyrins proposed by Gouterman[35] and by Petke *et al.* [41] for chlorins. When an electron withdrawing group is substituted on the porphyrin

macrocycle, the orbital most affected by this substitution should be the orbital which has the most charge at the substituent site. From Figure 9a it is obvious that the orbital most affected by meso substitution is the b_1 orbital. The c_1 and c_2 orbitals would also affected but not to as great a degree. The b_2 orbital with nodes at the meso positions is not anticipated to be strongly affected.

Gouterman's four orbital model predicts the basic intensity relationships in the absorption spectra by determining the degree of degeneracy between the top filled orbitals. Relative intensities of the Soret and Q transitions may be estimated by addition or subtraction of the transitions between the energy levels of the HOMO and LUMO orbitals (Figure 9b). Addition gives rise to the intense Soret transition while subtraction results in the much weaker Q bands. In porphyrin, the e_g orbitals (c_1 and c_2) are nearly degenerate while the a_{1u} (b_2) and a_{2u} (b_1) are not. When exactly degenerate, the $Q_{(0-0)}$ transitions should have zero intensity. The degeneracy can be broken in several ways. Addition of substituents to the ring, addition of the exocyclic ring V or reduction of the porphyrin macrocycle will break the symmetry and remove the degeneracy of the c_1 and c_2 orbitals. Chlorins have a lower symmetry, because of reduction of ring IV, than do porphyrins and the e_g orbitals lose their degeneracy. This accounts for the higher intensity of the Q transition in chlorins compared to porphyrins. In addition, when ring IV is reduced certain orbitals are affected more than others. The orbitals most affected by the reduction of ring IV are c_1 and b_2 because of the electron density located on ring IV. Reduction results in an increase in energy for these two orbitals which effectively removes the degeneracy of the c_1 and c_2 orbitals. The b_1 and

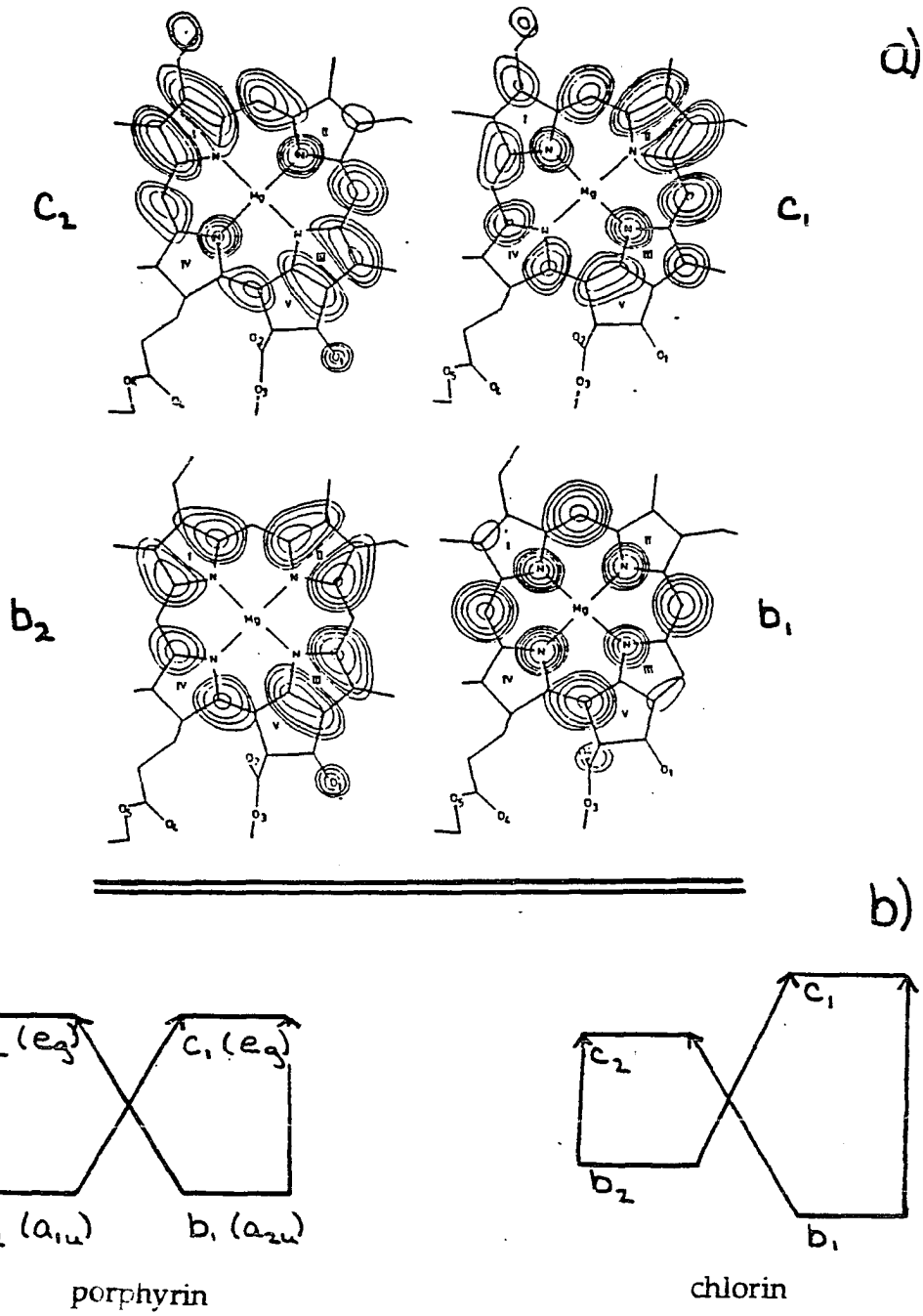

Figure 9. a) Electron density diagrams for chlorin
b) Relative energies of porphyrin and chlorin molecular orbitals

c_2 orbitals are only slightly affected. When the degeneracy is removed the intensity of the $Q_{(0-0)}$ transition increases.

The absorption transitions, in the visible region, have been assigned to two distinct electronic transitions, Q_x and Q_y. The assignments of the x and y polarization for these bands were based on analogy to the spectra of porphyrins and chlorins although the orthogonality of the transition dipoles was not supported by fluorescence measurements.[41] A recent publication by Fragata *et al.*[42], has reassigned some of the electronic transitions for chlorophyll. Their results substantiate the findings that the transitions are not orthogonal and suggest that several of the absorption bands are combinations of different transitions.

The absorption spectra for MPP *a* and its halogenated derivatives shown in Figure 2 have been normalized with respect to the Soret transition. The intensity of the $Q_{y(0-0)}$ transition for the X–MPP *a* series of compounds does not follow a consistent pattern for the series. The intensities are as follows: F < Br < H < Cl. The $Q_{y(0-1)}$ band decreases to approximately the same value for the halogenated compounds. However, the Q_x transitions do follow a pattern based on the size of the halogen substituent. The $Q_{x(0-0)}$ band increases on halogenation while the $Q_{x(0-1)}$ band decreases. In addition these bands are obviously red shifted. These results must be interpreted carefully because the intensity changes may be somewhat artificial due to the constraints imposed by normalization of the Soret band.

Early work reported by Bonnett *et al.* [19] dealt with monohalogenated porphyrins. Chlorination of octaethylporphyrin yielded two components, a mono– and di–chlorinated product. The monochlorinated compound was

halogenated at the α meso position. The absorption spectrum for this compound showed bathochromic shifts of all absorption bands, including the Soret band. The shifts appeared to be additive as the absorption peaks of the di–chloro derivative were shifted further to the red. Later work with symmetrically substituted porphyrins did not report red shifts of the absorption bands. In some cases a small blue shift is observed.[16,17,31,34,36] The blue shift is more pronounced when the halogen is substituted ortho to the macrocycle on the phenyl ring. In this case direct interaction of the halogen with the porphyrin ring occurs and the observed results are credited to an inductive effect of the halogen. In the case of the para substituted phenyl groups, the possibility exists for a resonance effect. It is most likely that an inductive effect has the strongest influence in these compounds with the halogen attached directly to the ring.

If the results observed for the symmetrically substituted porphyrins are also valid for the chlorin system, then the observed changes can be explained in terms of the four orbital model. The work of Kim *et al.* [31] with *ms*–TPP showed that an electron withdrawing group at the ortho position of the phenyl substituent raises the energy of the closest orbital by an inductive effect. A substituent directly attached to the ring at the meso position would raise the b_1 orbital in energy. The b_2 orbital would not be affected because there is no electron density at the meso positions. The c_1 and c_2 orbitals would also be expected to be raised in energy but not as much.

The intensity of the Q_x bands at 505 nm and 535 nm in MPP *a* are reversed after halogenation with the biggest change occurring in the brominated compound. This may be explained using Figure 9b. In MPP *a* the

Q_x transitions are almost equal in intensity. This correlates, in the diagram, to equal distance between b_1, c_2 and b_2, c_1. With halogenation,the orbital most affected is b_1. c_1, c_2 .and b_2 are affected to a lesser degree. The x transitions are no longer equal and this may account for the change in intensity. A different correlation may be obtained if the electronic transition assignments proposed by Fragata *et al.*[42] are used.

Electrochemistry

Electrochemical experiments were performed on MPP *a* and its derivatives. Half–wave potentials were measured as the average of the anodic and cathodic peaks and are listed in Table 4. Redox potentials for porphyrins depend on several different parameters. These include electronegativity and oxidation state of the central metal atom, dimer formation, number of axial ligands and basicity of the ring. It has been shown for porphyrins that as the basicity of the ring decreases oxidations become more difficult and reductions easier.[14,15,32] Electron withdrawing groups reduce the basicity of the ring and make oxidations more difficult. This is indeed the case with the halogenated compounds studied here. Once again, previous studies dealing with substituent effects on redox potentials employed symmetrically substituted metalloporphyrins; however the results reported agree with those obtained in previous work. $E_{1/2}$ was found to vary according to the Hammett equation:

$$E_{1/2} = \sigma\rho$$

The hydrogen "substituted" compound had the most negative oxidation potential which was in agreement with the substituent constant values, σ, (H) = 0.00, (F) = 0.06, (Cl) = 0.23, and (Br) = 0.23.[43] If ρ, the reactivity, is assumed to be constant for the four compounds, a reasonable assumption, then $E_{1/2}^{ox}$ observed would follow the trend predicted by the Hammett equation, which is indeed the case.

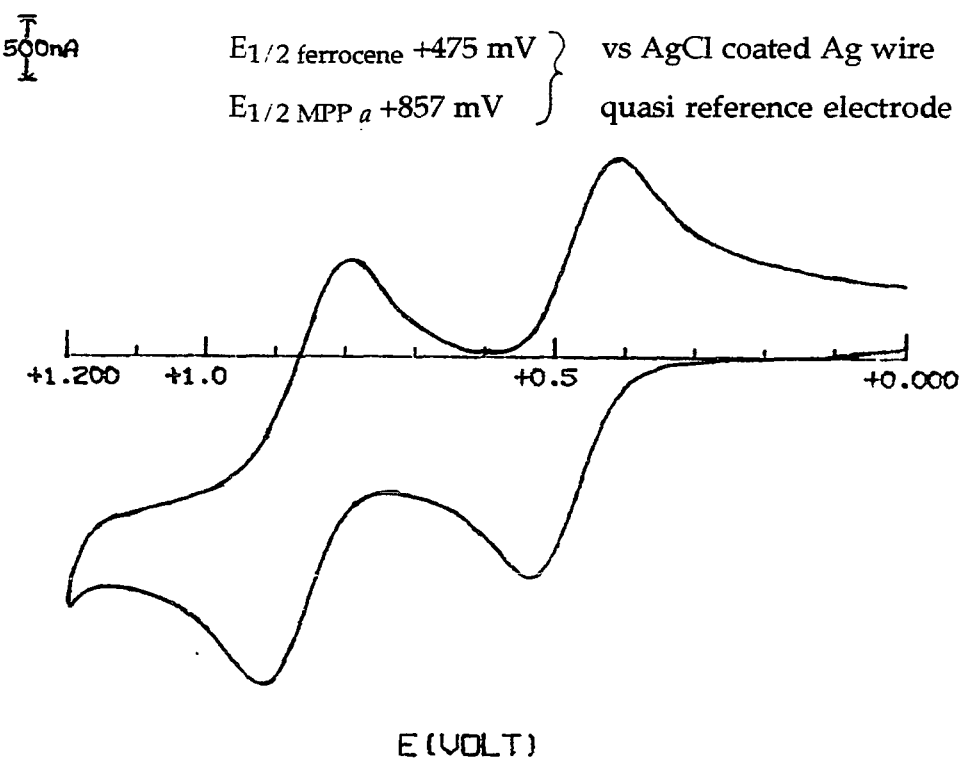

Figure 10. Cyclic voltammogram of MPP *a* and ferrocene (internal reference) in methylene chloride

NMR

The delta proton is missing from the NMR spectra of the halogenated compounds. All other protons are accounted for. Some of the proton shifts have moved either to higher or lower field strengths after halogenation. These shifts are due to the ring current effect in which the induced ring current is reduced. Protons in the plane of the ring experience a different ring current than protons either above or below the ring. Therefore if the ring current is affected by substitution of electron withdrawing groups onto the macrocycle then these protons will experience different effects.

Resonance Raman

Normal mode calculations have been carried out for Chl *a* and many model compounds,[28-30,37-39,44] Although mode assignments based on model compounds are useful, a cautious approach must be taken when correlating the results to a different system, as the normal mode composition may be changed. The resonance Raman spectra of the halogenated compounds are very similar to the parent compounds which suggests that halogenation does not greatly perturb the chlorin ring structure. However, certain changes are observed.

Substitution of a halogen for a hydrogen usually results in a downshift in the frequency associated with that vibration.[45] This is a well known effect and is the basis of identification of vibrational modes by isotopic substitution. In the compounds studied this would correspond to a decrease in the frequency of the C_aC_m mode at the δ-meso position. In addition, the $\delta C_mH(\delta)$

Table 5. Raman shift (in wavenumbers) on δ-halogenation.

H-MPPa	F-MPPa	Cl-MPPa	Br-MPPa	H-Pheo	Cl-Pheo	Br-Pheo	H-PPheo	Cl-PPheo	Br-PPheo	Assignment [a]
1702	1705	1706	1707	1713	1716	1715	1708	1711	1709	νCO(V)
1624	1623	1625					(1624)			$\nu C_aC_m(\alpha,\beta)$, $\nu C_aC_m(\delta)$[b]
1604	1605	1606	1606		1607	1607	1606	1607	1610	$\nu C_aC_m(\alpha,\beta)$
1579	1580	1580	1582	1581	1580	1580	1582	1581	1581	νC_aC_b(III), νC_bC_b(I)
1555	1551	1548	1548		1549	1551		1551	1547	νC_aC_b(III), νC_bC_b(I)
1535	1525	(1513)	(1513)		(1514)	(1514)		(1513)	(1512)	νC_bC_b(I), νC_aC_b(III), $\nu C_aC_m(\delta)$[b]
1500	1505	(1513)	(1513)	1497	(1514)	(1514)	1496	(1513)	(1512)	
1490	1489	1489	1489						1491	νC_aC_b(I), $\nu C_aC_m(\gamma)$[c]
1446	1447	1439		(1453)	1440	1440	1442	1435	1441	νCH_2(V) scissors, $\nu C_aC_m(\gamma,\delta)$, νC_aC_b (I, II, III)
1406	1403	1409	(1406)	1409	1412	1409	1408	1411	1411	
1264	1259	1265	1268	1264	1264	1268	1265	1268	1265	$\delta C_mH(\alpha,\beta)$
1223	1226	1226	1228	1225	1227	1227	1223	1225	1228	δC_bH(IV), δCH_2(V-9) wag, δC_nH (δ)
1026	1030	1030	1042	1033	1038	1040	1028	1033	1036	$\delta C_mC_aC_b$ (I, II, III)

[a]Assignments are from Boldt *et al.*[39] and Fujiwara and Tasumi.[44]

[b]Assignments based on results from these experiments.

[c]Calculated vibrational mode from Boldt *et al.*[39]

band should disappear and a new band corresponding to a $\delta C_mCl(\delta)$ in the low frequency region, 650 to 750 cm^{-1} should appear. If a localized model for the halogenated compounds is assumed, then halogen substitution would also affect those bands associated with core size, C_aN and C_aC_b on rings I and IV, It is obvious that the same bands are affected in each of the halogenated series, therefore, unless otherwise noted, the changes discussed will be for MPP *a* and its halogenated derivatives.

No new bands which could be assigned to a $\delta C_mCl(\delta)$ bend were observed in the spectra of the halogenated compounds with 406.7 nm excitation. This transition may not have been resonantly enhanced at this wavelength and it may be that at a different excitation wavelength, e.g., within one of the Q transitions which shows a large change on halogenation, this vibration will be observed.

The shoulder band at 1624 cm^{-1}, which shifts to slightly lower frequency upon halogenation,is assigned as a $C_aC_m(\alpha,\beta)$ stretch.[39,44] The vibration due to the $C_aC_m(\delta)$ is expected to undergo a downshift in frequency with addition of the halogen; in a localized system, the C_aC_m vibrations for the α and β methine bridges should not be affected in this manner. This band may therefore contain some contribution from the $\nu C_aC_m(\delta)$ vibration.

The intensity of the band at approximately 1607 cm^{-1}, also assigned to $\nu C_aC_m(\alpha,\beta)$, increases with halogenation but the band does not experience a frequency shift. This supports the tentative assignment for a contribution from $C_aC_m(\delta)$ to the 1624 cm^{-1} band. The increased intensity of the 1607 cm^{-1} band in the halogenated derivatives may be due to the combination of two

different vibrations, i.e., the 1624 cm^{-1} band is shifted to lower frequency and shifts underneath the 1607 cm^{-1} band.

The 1550 cm^{-1} band becomes more distinct with halogenation. In the brominated compounds it is a definite peak and not just a shoulder as in the parent compound. This has been assigned to a stretching vibration of C_aC_b(III) and C_bC_b(I).

The band at 1535 cm^{-1} in MPP *a* , assigned by Boldt *et al.*[39] as νC_bC_b(I), νC_aC_b(III), may be downshifted to 1514 cm^{-1} in the halogenated derivatives. From the observed downshift, the data suggest that there may also be a contribution from a mode involving the δ meso position. The band at approximately 1500 cm^{-1}, in the parent compounds, appears to upshift by about 5, 12, and 14 cm^{-1} for the fluorinated, chlorinated and brominated derivatives respectively. The calculated assignment[39, 44] for this vibration is νC_aC_b(I), $\nu C_aC_m(\gamma)$. There is a small band, somewhat difficult to distinguish, at approximately 1490 cm^{-1} that does not change in frequency. This has been assigned to $\nu C_aC_m(\delta)$ and νC_aC_b(I) vibrations. The results presented here, suggest that this mode may contain vibrations due mainly to νC_aC_b(I).

Other changes that are noted in the spectra of the halogenated derivatives occur in the low frequency region. The band at 789 and 777 cm^{-1} in MPP *a* split apart in the derivative compounds and the relative intensity changes between the two peaks. The low frequency region has not been as well characterized as the high frequency region but these modes have been assigned as pyrrole breathing modes. It is not possible to say more about these assignments at this time.

CONCLUSIONS

The primary objectives of this work were to synthesize specifically derivatized chlorophylls and to characterize these compounds as fully as possible. Addition of a halogen to the chlorin macrocycle induced changes in the physical and chemical properties with respect to the parent compounds. Some of these changes were expected, e.g., the electrochemistry followed the Hammett equation for change in redox potential with substitution. Other changes did not follow the expected behavior based on previous studies, e.g., the red shifts of the Q bands in the absorption spectra. These shifts have been explained to our satisfaction, however. It was thought that the Raman spectra of these compounds would show larger changes than were actually observed. In addition, some of the assignments based on normal coordinate analysis are not consistent with our observations. This may be due to the fact that the original composition of the affected bands is not maintained upon halogenation.

ACKNOWLEDGEMENT

This work was funded by US Department of Energy Grant No. 84ER13261. I wish to thank Dr. Tomaz Michalski at Argonne National Laboratory for his help with the synthesis of the halogenated derivatives.

REFERENCES

(1) Gust, D.; Moore, T. A. In *Photoinduced Electron Transfer III*; J. Mattay, Ed.; Springer-Verlag: New York, 1991; pp 103-151.

(2) Watanabe, T.; Kobayashi, M.; Hongu, A.; Nakazato, M.; Hiyama, T.; Murato, N. *FEBS Letters* **1985**, *191*, 252-256.

(3) Dörnemann, D.; Senger, H. *Photochem. Photobiol.* **1982**, *35*, 821-826.

(4) Katoh, T.; Dörnemann, D.; Senger, H. *Plant Cell Physiol* **1985**, *26*, 1583-1586.

(5) Senger, H.; Dörnemann, D.; Dotzabasis, K.; Senge, M.; Schmidt, W.; Wissenback, M. In *Progress in Photosynthesis Research*; J. Biggens, Ed.; Martinus Nijhoff Publishers: Dordrecht, 1987; Vol. IV; pp 491-398.

(6) Scheer, H.; Gross, E.; Nitsche, B.; E., C.; Schneider, S.; Schäfer, W.; H.-M., S.; Schulten, H.-R. *Photochem. Photobiol.* **1986**, *43*, 559-571.

(7) Kobayashi, M.; Watanabe, T.; Struck, A.; Scheer, H. *FEBS Letters* **1988**, *235*, 293-297.

(8) Senge, M.; Senger, H. *Photochem. Photobiol.* **1988**, *48*, 711-717.

(9) Senge, M.; Dörnemann, D.; Senger, H. *FEBS Letters* **1988**, *234*, 215- 217.

(10) Senge, M.; Struck, A.; Dörnemann, D.; Scherr, H.; Senger, H. *Z. Naturforsch* **1988**,

(11) Senge, M.; Senger, H. In "*Proceeding from New Developments and Techniques in Photosynthesis*"; J. Barber, Ed.; 1988.

(12) Gouterman, M. *J. Chem. Phys.* **1959**, *30*, 1139-1161.

(13) Hynninen, H.; Lötjönen, S. *Tetrahedron Lett.* **1981**, *22*, 1845-??

(14) Kadish, K. M.; Morrison, M. M.; Constant, L. A.; Dickens, L.; Davis, D. G. *J. Am. Chem. Soc.* **1976**, *98*, 8387-8390.

(15) Kadish, K. M.; Morrison, M. M. *Bioinorg. Chem.* **1977**, *7*, 107-115.

(16) Shellnutt, J. A. *J. Phys. Chem.* **1984**, *88*, 4988-4992.

(17) Shellnutt, J. A.; Ortiz, V. *J. Phys. Chem.* **1985**, *89*, 4733-4739.

(18) Woodward, R. B.; V., S. *J. Am. Chem. Soc.* **1961**, *83*, 4676-4678.

(19) Bonnett, R.; Gale, A. D.; Stephenson, G. F. *J. Chem. Soc. (C)* **1966**, 1600-1604.

(20) Bonnett, R.; Chaney, B. D. *J. Chem. Soc. Perkin Trans. I* **1987**, 1063-1067.

(21) Bonnett, R.; Campion-Smith, I. H.; Kozyrev, A. N.; Mironov, A. F. **1989**,

(22) Strain, H. H.; Svec, W. A. In *The Chlorophylls*; L. P. Vernon and G. R. Seely, Ed.; Academic Press: New York, 1966.

(23) Smith, K. M.; Simpson, D. J. *J. Am. Chem. Soc.* **1985**, *107*, 4946-4954.

(24) Michalski, T. J.; Appleman, E. H.; Bowman, M. K.; Hunt, J. E.; Norris, J. R.; Cotton, T. M.; Raser, L. *Tetrahedron Letters* **1990**, *31*, 6847-6850.

(25) Minnetian, O. M.; Morris, I. K.; Snow, K. M.; Smith, K. M. *J. Org. Chem.* **1989**, *54*, 5567-5574.

(26) Tasumi, M.; Fujiwara, M. In *Spectroscopy of Inorganic-based Materials*; R. J. H. Clark and R. E. Hester, Ed.; John Wiley & Sons: New York, 1987; pp 407-428.

(27) Lutz, M. In *Advances in Infrared and Raman Spectroscopy*; R. J. H. Clark and R. E. Hester, Ed.; Wiley Heyden: New York, 1984; Vol. 11; pp 211-300.

(28) Li, X.-Y.; Czernuszewicz, R. S.; Kincaid, J. R.; Spiro, T. G. *J. Am. Chem. Soc.* **1989**, *111*, 7012-7023.

(29) Li, X.-Y.; Czernuszewicz, R. S.; Kincaid, J. R.; Su, Y. O.; Spiro, T. G. *J. Phys. Chem.* **1990**, *94*, 31-47.

(30) Li, X.-Y.; Czernuszewicz, R. S.; Kincaid, J. R.; Stein, P.; Spiro, T. G. *J. Phys. Chem.* **1990**, *94*, 47-61.

(31) Kim, J. B.; Leonard, J. J.; Longo, F. R. *J. Am. Chem. Soc.* **1972**, *94*, 3986-3992.

(32) Kadish, K. M.; Morrison, M. M. *Inorg. Chem.* **1976**, *15*, 980-982.

(33) Moet-Ner, M.; Adler, A. D. *J. Am. Chem. Soc.* **1975**, *97*, 5107-5111.

(34) Longo, F. R.; Finarelli, M. G.; Kim, J. B. **1969**, 927-931.

(35) Gouterman, M. *J. Molec. Spectros.* **1961**, *6*, 138-163.

(36) Spellane, P. J.; Gouterman, M.; Antipas, A.; Kim, S.; Liu, Y. C. *Inorg. Chem.* **1980**, *19*, 386-391.

(37) Abe, M.; Kitagawa, T.; Kyogoku, Y. *J. Chem. Phys.* **1978**, *69*, 4526-4534.

(38) Atamian, M.; Donohoe, R. J.; Lindsey, J. S.; Bocian, D. F. *J. Phys. Chem.* **1989**, *93*, 2236-2243.

(39) Boldt, N. J.; Donohoe, R. J.; Birge, R. R.; Bocian, D. F. *J. Am. Chem. Soc.* **1987**, *109*, 2284-2290.

(40) Katz, J. J.; Shipman, L. L.; Cotton, T. M.; Janson, T. R. In *The Porphyrins*; D. Dolphin, Ed.; Academic Press: New York, 1978; Vol. V; pp 401-458.

(41) Petke, J. D.; Maggiora, G. M.; Shipman, L.; Christoffersen, R. E. *Photochem. Photobiol.* **1989**, *00*, 1-22.

(42) Fragata, M.; Norden, B.; Kurucsev, T. *Photochem. Photobiol.* **1988**, *47*, 133-143.

(43) Hansch, C.; Leo, A. *Substituent Constants for Correlation Analysis in Chemistry and Biology*; John Wiley & Sons: New York, 1979.

(44) Fujiwara, M.; Tasumi, M. *J. Phys. Chem.* **1986**, *90*, 5646-5650.

(45) Dollish, F. R.; Fateley, W. G.; Bentley, F. F. *Characteristic Raman Frequencies of Organic Compounds*. John Wiley & Sons: New York, 1974.

SECTION II. FACTORS DETERMINING STABILITY OF BACTERIOCHLOROPHYLL MONOLAYERS

ABSTRACT

The important chemical and physical factors determining the integrity of bacteriochlorophyll monolayers must be identified in order that this pigment can be of maximum value and reliability when monolayer and multilayer structures are used for model systems of the in vivo photosynthetic process. This study identifies these factors and characterizes major decomposition products. Spread monolayers of bacteriochlorophyll were subjected to variation of pH, temperature, subphase composition, incident light flux and atmospheres of various composition. Results were consistent with intuitional prediction as well as known behavior of monolayers of chlorophyll a. Minimal decomposition was noted under conditions of darkness, presence of reducing agents either in the subphase or as an integral part of the monolayer, subambient temperatures, inert atmospheres (e.g., nitrogen) and alkaline subphase pH. Cognizance of the importance of these parameters and their control during monolayer manipulations of bacteriochlorophyll will result in optimum monolayer model systems of assured purity.

INTRODUCTION

This study identifies the important chemical and physical factors which determine the stability and integrity of bacteriochlorophyll (BChl) monolayers. In addition, the structures of major degradation products have been determined. This information is essential for extension of monolayer techniques to the use of this important photosynthetic pigment for preparing model systems, based on monolayer techniques and Langmuir–Blodgett constructions. Incorporation of BChl into synthetic membrane systems to simulate the photoinduced electron transfer seen in bacterial photosynthesis presents potential difficulties. In a native membrane, the BChl (or Chl) pigments are quite stable; however, the isolated pigments removed from the native environment are prone to degradation reactions. Early work by Brody[1] indicated that Bchl monolayers are more unstable than those of Chlorophyll *a* (Chl *a*), the more widely studied pigment of green plants. Brody chemically oxidized BChl *a* in bulk and suggested that the changes seen in BChl monolayers should be associated with this oxidation product. Kim[2] has studied the various degradation products that were formed when BChl is subjected to repeated chromatography using sucrose columns.

If synthetic systems containing photosynthetic pigments are to be constructed so as to mimic native systems, degradation of pigments must be minimized, if possible. The identity of any degraded products that may form should be known. In the present study, spread monolayers were subjected to a variety of conditions thought to be important in influencing the chemical integrity of BChl. The effects of the following factors were studied: subphase pH; oxygen content of the atmosphere over the monolayer; the subphase,

temperature, irradiation, and the influence of antioxidants both dissolved in the subphase and present as an integral component of the monolayer. In addition,the putative degradation products were synthesized and these were compared with the actual compounds collected from the monolayer trough after experiments. Several analytical techniques were utilized to identify the degradation products; these include absorption and surface-enhanced resonance Raman scattering (SERRS) spectroscopies, reverse phase (r.p.) HPLC and NMR.

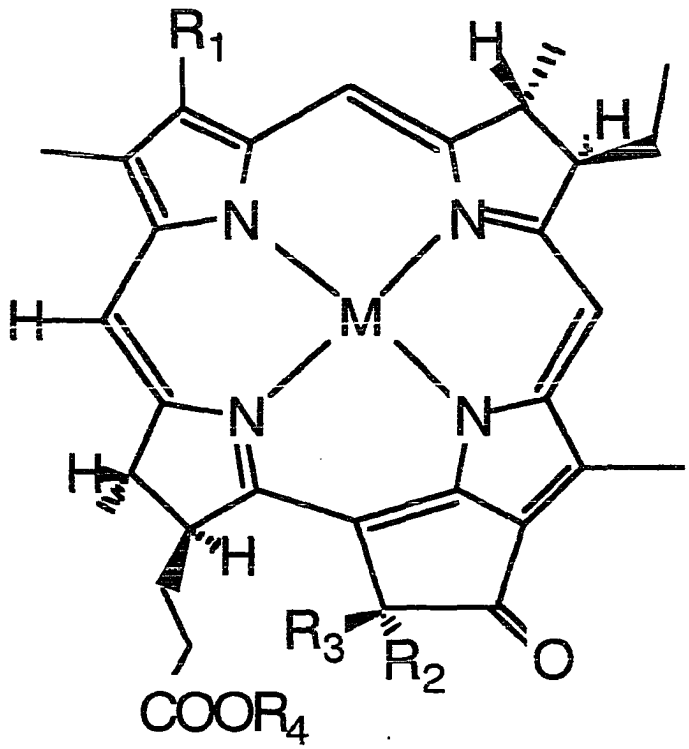

Compound	M	R_1	R_2	R_3	R_4
Bchl *a*	Mg	$COCH_3$	H	$COOCH_3$	$C_{20}H_{39}$
"X"-BChl *a*	Mg	$COCH_3$	OH	$COOCH_3$	$C_{20}H_{39}$
Ox. BChl *a*	Mg	$CHCH_2$	H	$COOCH_3$	$C_{20}H_{39}$
BPheo *a*	2H	$COCH_3$	H	$COOCH_3$	$C_{20}H_{39}$
MeBPheo *a*	2H	$COCH_3$	H	$COOCH_3$	CH_3

Figure 1. Structure of BChl *a* and degradation products

EXPERIMENTAL METHODS

Monolayers

Monolayers were formed by spreading a chloroform solution of BChl a followed by compression to a surface pressure of 20 mN/m. The monolayers were then left undisturbed for 2 hours. The following parameters were varied systematically, with all variables held constant except for the specific one under study: [1] Composition of the atmosphere over the monolayer (subphase water was previously equilibrated with the same gas), which was either air, nitrogen or oxygen. [2] Composition of subphase, which was either pure monolayer–grade water, phosphate buffer at pH 7.0 or 8.0, or these subphases with or without sodium ascorbate (10^{-3} molar). [3] Monolayer composition, i.e. either pure BChl a or added ascorbyl palmitate (15 mole–per cent). [4] Temperature – 12, 18, 25, or 40 C. [5] Light conditions – total darkness,green safety light (1.4×10^{-5} w/cm^2), fluorescent light (4.6×10^{-3} w/cm^2) or actinic incandescent light (2.2×10^{-2} w/cm^2). After an experiment, the monolayer was collapsed by compression of Teflon barriers. The monolayers were collected and subjected to high performance liquid chromatography (HPLC).

HPLC and SERRS

Originally a Ultrex 3 μ C_{18} (75 x 4.6 mm) analytical column was employed. The mobile phase was acetonitrile/methanol (3:1) with a flow rate of 1 ml/min. Detection of eluents was by a uv–visible flow detector set at 400 nm. The retention times and separation efficiency under these conditions was poor. Therefore, the column was changed to a Nova–Pak 4 μ C18 (150 x

3.9 mm) with mobile phase of ethanol/water (86:14), flow rate of 0.75 ml/min, λ_{det} = 380 nm. Separation with this system was much improved.

The four most probable BChl decomposition products were synthesized, isolated by r.p. HPLC, and the SERRS spectra collected. The five compounds, including non-degraded BChl *a*, were: [1] BChl *a*: extracted from chromatophores[3]; [2] BPheophytin *a* (BPheo *a*): by acidification of BChl *a*; [3] Methyl BPheophorbide *a* (MeBPheo *a*): reaction of BChl *a* in 5% H_2SO_4 in MeOH for 12 hours at room temperature; [4] oxidized BChl *a*: extraction of BChl *a* with p–chloranil in acetone; [5] "X"–BChl *a*: most likely 10–OH BChl *a*, formed upon standing in the HPLC mobile phase with ethanol. These five compounds were purified individually by HPLC. With these, the individual retention times were determined. The five compounds were mixed together and reinjected into the HPLC to ensure that there were no overlapping of eluting bands (Figure 1). Individually purified compounds were collected and the solvent evaporated in a nitrogen stream. For SERRS spectral identification, the material was redissolved in diethyl ether and adsorbed onto an electrochemically roughened silver electrode. SERRS experiments were carried out at 77 K using the 406.7 nm line of a Coherent Innova 100 Kr^+ laser. Power at the sample was approximately 15 mw. The scattered radiation was collected in a backscattering geometry with a 60° angle. Experimental conditions have been described elsewhere.[4]

RESULTS AND DISCUSSION

Under conditions for which maximum decomposition was noted, the HPLC chromatogram indicated five major decomposition products, the most abundant of which was 2'-desvinyl chlorophyll *a*. This had previously been described by Brody (1). Decomposition increased progressively with increasing temperatures (12 C to 40 C). Low pH conditions favored formation of bacteriopheophytin by magnesium removal. Decomposition was greater in a pure oxygen atmosphere, much less in a nitrogen atmosphere. Highest stability was attained in complete darkness,and maximum decomposition occurred with irradiation utilizing fluorescent light and oxygen. Use of a green safety light resulted in decreased decomposition. The presence of the antioxidant greatly reduced decomposition products formed, when it was present either dissolved in the subphase (sodium ascorbate) or present as a monolayer component (ascorbyl palmitate).

Less than 0.5% degradation of BChl a was observed when the monolayer structure was maintained for more than one hour under the following conditions: subphase temperature 15 C; atmosphere of N_2; subphase pH 7.0 in phosphate buffer (0.20M) in the presence of sodium ascorbate (2.0×10^{-3} M) and a green safety light.

HPLC

The retention times for the five compounds are as follows: MeBPheo *a*: 2.5 min; "X"-BChl *a*: 9.8 min; BChl *a*: 10.4 min; Ox. BChl *a*: 11.8 min;BPheo *a*: 25.5 min. The retention times differ sufficiently for identification of each compound. In addition, the separation between eluting components is

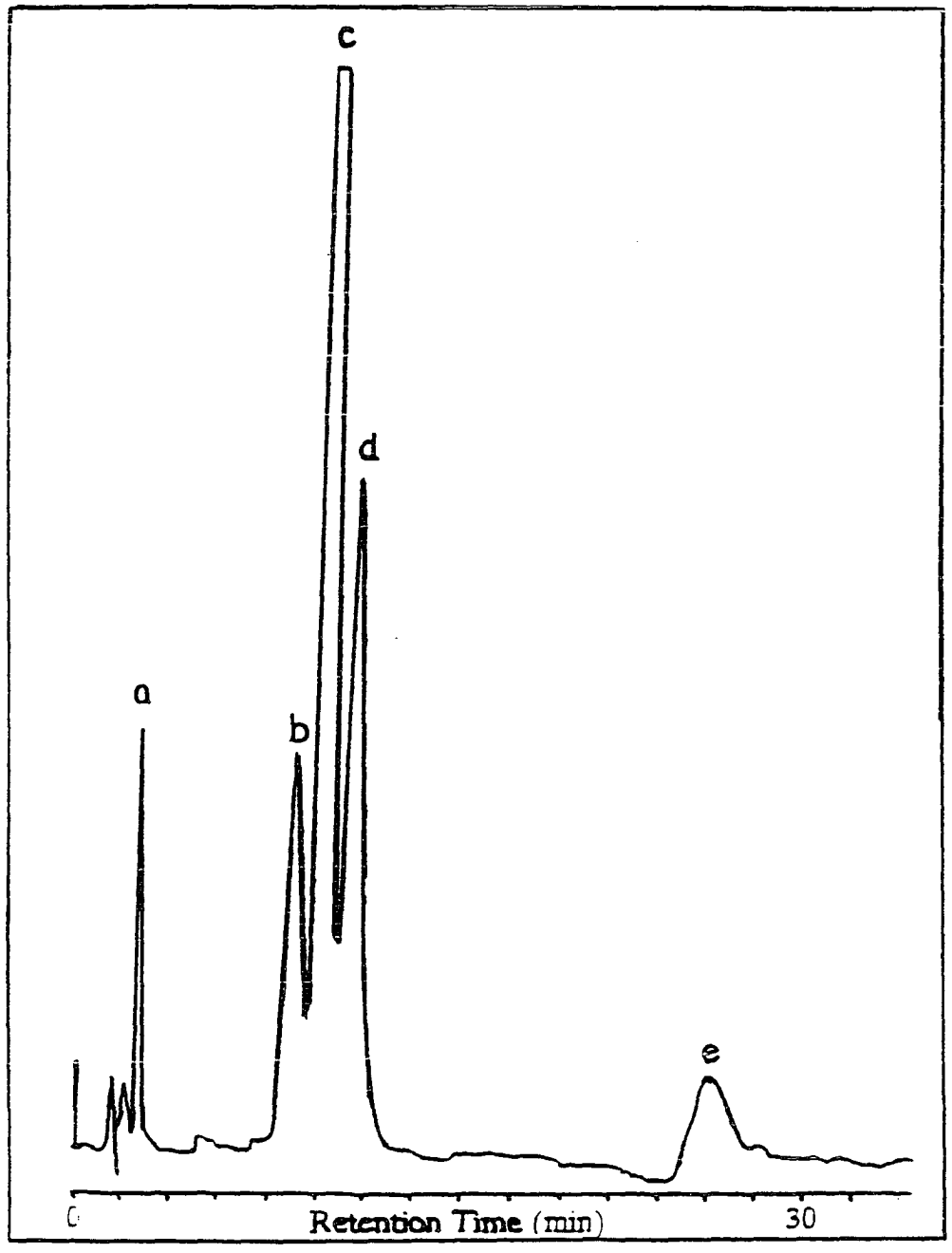

Figure 2. HPLC chromatogram of a) MeBPheo *a*, b) "X"–BChl *a*, c) BChl *a*, d) Ox. BChl *a*, and e) BPheo *a*. Nova–Pak 4 μm, C_{18}; flow rate 0.75 ml/min; EtOH/H_2O (86:14)

sufficiently large that collected fractions from the HPLC contain only one component. The samples were later used for the SERRS experiments.

SERRS

The absorption spectra (Perkin Elmer Lambda 6 UV/Visible Spectrophotometer) are shown in Figure 2 and the SERRS spectra of BChl *a* and the synthesized degradation products are shown in Figure 3. The Raman shifts and corresponding assignments are listed in Table 1. The SERRS spectra for BChl *a* and X–BChl *a* are very similar although the carbonyl modes at 1700 and 1655 cm^{-1} are more obvious in the latter; the bands at 1556 and 1341 cm^{-1} are also more pronounced. The optical absorption spectra of the two compounds are quite similar; therefore little difference in the resonance Raman spectra would be expected under the resonance conditions used. The spectra of oxidized BChl *a* resembles that of Chl *a*, with the most intense band located at 1556 cm^{-1} rather than 1611 cm^{-1}. Also, a large shoulder at 1533 cm^{-1} appears that is a minor peak in the BChl *a* spectrum. In addition, two new bands also appear at 1235 and 1496 cm^{-1}. There are some obvious differences in the spectra of BChl *a* and the demetallated products. The band at approximately 1583 cm^{-1} becomes more intense as do the bands at 1368 and 1213 cm^{-1} and the peak at 1530 cm^{-1} shifts to 1548 cm^{-1}. The 1285 cm^{-1} band disappears and a new vibrational band is seen at 1307 cm^{-1} in the pheophytin spectra.

Of the model compounds synthesized, the structure of two compounds was initially unknown. From literature references,[5] the compound called Ox. BChl *a* is probably 2'–desvinyl Chl *a*. The absorption spectra of this

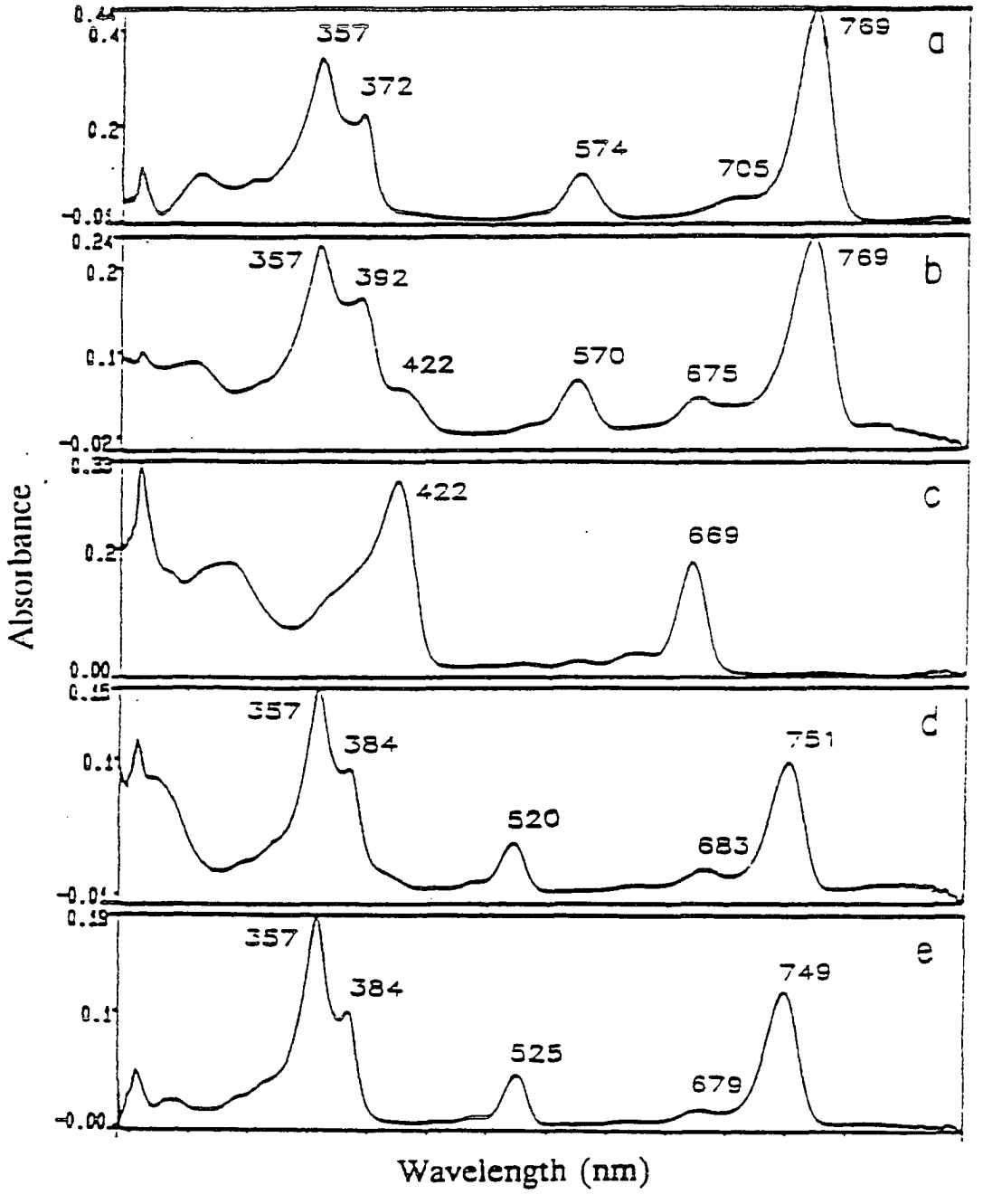

Figure 3. Absorption spectra of a) BChl *a*, b) "X"–BChl *a*, c) Ox. BChl *a*, d) MeBPheo *a*, and e) BPheo *a* in ether

compound closely resembles that of a chlorin rather than a bacteriochlorin (i.e. the Q_y maximum is at 660 nm instead of 760 nm as is the case for BChl *a*). NMR should indicate conclusively if this is the case. The second compound of interest is "X"–BChl *a*; the absorption spectrum of which is very similar to BChl *a* with the exception of an increased absorption in the Q_y region at 676 nm, a shoulder appears around 423 nm and a small blue shift of the Q_x band from 574 to 571 nm. This compound is readily formed by letting a solution of BChl *a* in ethanol stand for a period of several hours. Kim[2] had suggested that this compound might be a precursor to the fully oxidized product; however, Struck[6] studied several different BChl *a* degradation products and determined that this compound was 10–OH BChl *a*. As this compound was formed by standing in an ethanol solution (synthesis also used by Struck), and our results with absorption spectroscopy and with NMR (not shown) are in agreement with his data, we have concluded that "X"–BChl *a* is quite probably 10–OH BChl *a*.

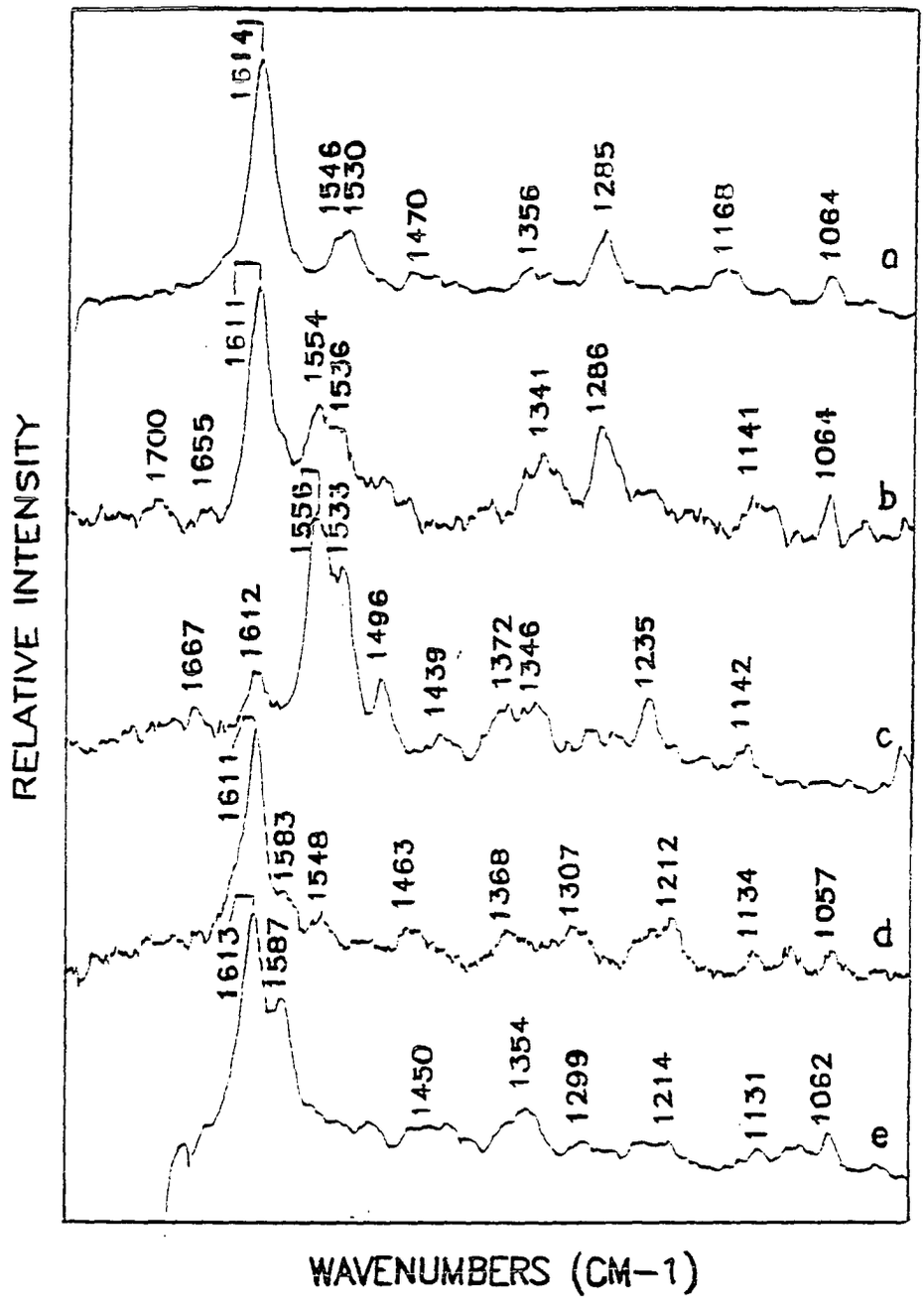

Figure 4. SERRS spectra of a) BChl *a*, b) "X"–BChl*a*, c) Ox. BChl *a* d) BPheo *a*, and e) MeBPheo *a*.77 K; integration time, 30 sec; spectral resolution, 1 cm^{-1}.

Table 1. SERRS assignments (in wavenumbers, cm^{-1}) of BChl *a* and degradation Products with 406.7 nm excitation. Laser power, 20 mW; integration time, 30 sec; spectral resolution, 4 cm^{-1}

BChl *a*	"X"-BChl *a*	OxBChl *a*	BPheo *a*	MeBPheo *a*	Assignment[a]
	1700	1685			C0(V)
	1655	1667			
1614	1611	1612	1611	1613	C_aC_m
1583	1589		1583	1587	C_aC_b
1546	1554	1556	1548		C_bC_b
1530	1536	1533			C_aC_b
		(1376)	1368	1376	C_aN
1285	1286	1291			C_mH
	1141	1142	1134	1131	C_aN
1064	1043	1064	1057	1062	C_aN

[a]Assignments are from references (4,7,8).

CONCLUSIONS

Several conclusions may be drawn from this study. BChl *a* decomposes with formation of multiple degradation products, even under mild conditions. The products are difficult to identify by their optical absorption spectra alone. Monolayers of BChl *a* undergo minimal degradation when conditions are such that oxidative situations are avoided. However, for the degradation products formed, SERRS was demonstrated to be a valuable technique for identification of low concentration of decomposition products when used in conjunction with analytical HPLC.

ACKNOWLEDGEMENT

This work was supported in part by the US Department of Energy, Office of Chemical Sciences.

REFERENCES

1. S. S. Brody, *Z. Naturforsch,* **266** (1971a) 134.
2. W. S. Kim, *Biochim. Biophys. Acta,* **112** (1966) 39
3. H. H. Strain and W. A. Svec, in Leo P. Vernon and Gilbert R. Seeley, (eds.), *The Chlorophylls,* Academic Press, New York, 1966, pp 58–59.
4. P. M. Callahan and T. M. Cotton, *J. Am. Chem. Soc. 109* (1987) 7001.
5. P. S. Reinach, *Bacteriochlorophyllous and Cytochrome c Monomolecular Films at Air–Water Interfaces as Models for Membrane Phenomena,* Ph.D. Dissertation, 1972, New York University.
6. A. Struck, *Chemisch modifizierte Bakteriochlorophylle und –pheophytine in den Bindungsstellen $B_{A,B}$ und $H_{A,B}$ von photosynthetischen Reaktionszentren aus Rhodobacter sphaeroides R26: Pigmentsynthese, Pigmentaustausch und Spektroskipie.* Ph.D. Dissertation, 1990, Ludwigs–Maximilians–Universitt, Munche.
7. M. Lutz, In R. J. H. Clark and R. E. Hester (eds.) *Advances in Infrared and Raman Spectroscopy,* Vol. 11, Wiley, New York, 1984, pp 211–300.
8. N. J. Boldt, R. J. Donohoe, R. R. Birge and D. F. Bocian, *J. Am. Chem. Soc. 109* (1987) 2284.

SECTION III. RESONANCE RAMAN AND SURFACE ENHANCED RESONANCE RAMAN CHARACTERIZATION OF HYPERICIN AND RELATED COMPOUNDS

ABSTRACT

Hypericin has been found to exhibit a variety of photodynamic effects. To correlate biological activity with molecular structure, complete physical characterization of hypericin is required. The vibrational spectrum has been determined and resonance Raman and surface-enhanced resonance Raman scattering (SERRS) spectra are reported. In addition, the Raman spectra of model compounds have been determined to facilitate assignment of the vibrational modes of hypericin.

INTRODUCTION

Hypericin (structural formula, Fig. 1), a multi-ring quinoidal compound found in certain species of the plant genus *Hypericum*, has been shown to exhibit a variety of photodynamic effects (Blum, 1941; Pace and MacKinney, 1941; Knox and Dodge, 1985; Duran and Song, 1986; Knox *et al.*, 1987). Hypericism, a condition of severe sensitivity to light, was observed in a variety of animals after ingestion of hypericin containing plants (Pace, 1942; Brockmann, 1952; Thomson, 1971; Giese, 1971 and 1980). In addition to inducing photosensitivity, it was discovered that hypericin is the chromophore of the photoreceptor (stentorin) that is responsible for the negative phototactic response of *Stentor* (Song *et al.*, 1980; Walker *et al.*, 1986; Yang *et al.* 1986). It is also known to have bactericidal properties and was used at one time as an antidepressant (Duran and Song, 1986). Recent findings that hypericin shows a photodynamic effect against several retroviruses, including HIV, has made it essential that this compound and its mode of action be understood as fully as possible (Carpenter and Kraus, 1991; Hudson *et al.*, 1991; Lopez-Bazzocchi *et al.*, 1991).

The photodynamic action of hypericin is thought to be the result of either the formation of radicals, a Type I mechanism, or through the formation of singlet oxygen, a Type II mechanism. Both mechanisms have been observed in *in vitro* studies (Heitz, 1987; Knox *et al.* , 1987). The singlet oxygen quantum yield for hypericin has been determined and is quite large, 0.74 (Jardon *et al.*, 1986; Jardon *et al.*, 1987). A value such as this indicates an efficient intersystem crossing mechanism, common for aromatic ketones, involving conformational changes (difficult in the rigid hypericin structure)

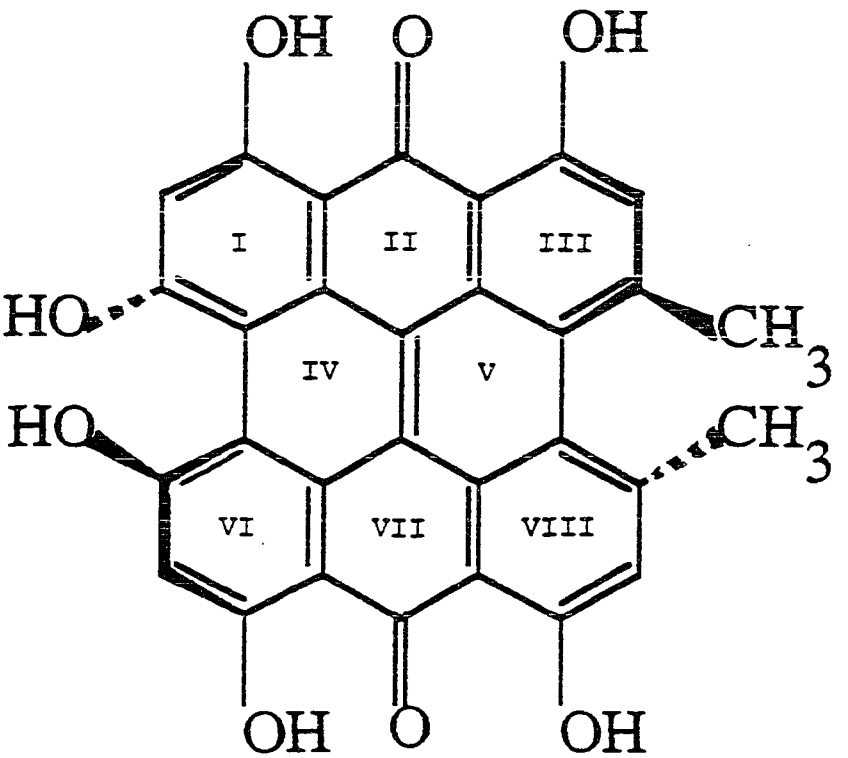

Figure 1. Structure of hypericin

or aggregation (Turro, 1978). The high triplet yield suggests significant electron density is present on the carbonyls of hypericin in the excited state. Before a complete understanding of the mode of action is possible, the relevant physical, chemical and biological parameters must be established. Absorption, fluorescence and phosphorescence spectra of hypericin have been previously reported (Pace and Mackinney, 1939; Scheibe and Schontag, 1942; Walker *et al.*, 1979; Jardon *et al.*, 1986; Jardon *et al.*, 1987; Racinet *et al.*, 1988; Jardon and Gautron, 1989).

In this study, Raman spectroscopy was employed to elucidate the vibrational spectrum of hypericin and various analogs. Raman spectroscopy has several advantages compared to IR for biological studies, the most important being the lack of interference from water. Also, visible wavelengths are used in Raman and, therefore, no special optics or sample containers are needed. The vibrational and other physical data for hypericin are essential for complete characterization of hypericin in order to correlate the biological activity with the molecular structure. Surprisingly, little work has been done in this area and, therefore, studies on model compounds are necessary. In addition, absorption experiments, designed to assess the amount of aggregation, were also performed.

Two variations of Raman spectroscopy have been utilized in this study. These are resonance Raman (RR) and surface–enhanced resonance Raman scattering (SERRS) spectroscopy. The resonance effect arises when the wavelength of light used for Raman excitation is in resonance with an electronic absorption band, resulting in enhancement of the vibrational modes that are coupled to that transition. This enhancement can be as high

as 10^6 fold. Surface enhancement arises when a molecule is adsorbed onto a roughened metal surface (most often Ag, Au or Cu). The roughened metal gives rise to an increase Raman scattering thru either an electromagnetic or a chemical enhancement mechanism. Often, a decrease in fluorescence also occurs and this leads to a further increase in the signal to noise ratio (Cotton, 1988).

In any application of SERRS, it is necessary to consider the nature of the molecule–surface interactions. In these experiments, the Raman spectrum of solid hypericin was compared with the solution SERRS spectrum to determine whether a strong chemical interaction is present between hypericin and the Ag surface. If such were the case, the surface spectrum should exhibit large shifts and intensity changes for some bands as compared to the RR spectrum.

Raman spectra of several analogs have also been studied in an effort to assign the vibrational modes of hypericin. The analogs studied include anthracene, A; 9,10–anthraquinone, AQ; 9,10–phenanthrenequinone, PQ; anthraflavic acid (2,6–dihydroxy–9,10–anthraquinone), AF; and emodin (1,3,8–trihydroxy–6–methyl–9,10–anthraquinone), E. Structures for these compounds are shown in Figure 2. The Raman and SERS (surface enhanced Raman scattering) spectra of the model compounds were obtained and compared with hypericin. With the exception of emodin, the excitation wavelengths were not in resonance with any electronic transition in these model compounds. At present a detailed analysis of the vibrational modes of hypericin is not possible; however, some general conclusions may be drawn.

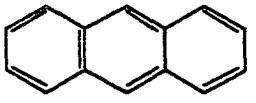

Anthracene

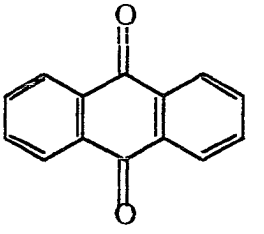

9,10-Anthraquinone

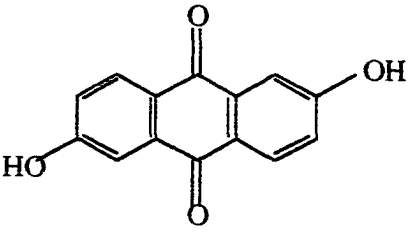

Anthraflavin

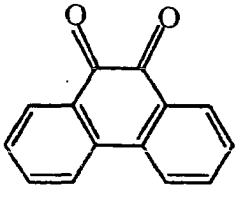

9,10-Phenanthrenequinone

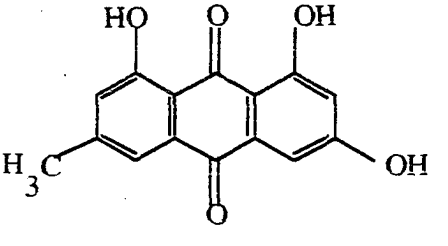

Emodin

Figure 2. Structures of hypericin analogs

MATERIALS AND METHODS

The hypericin was synthesized and purified in Dr. G. Kraus' laboratory at Iowa State University. Model compounds were used as received (Aldrich, Milwaukee, WI) except for anthraflavin and 9,10–phenanthrenequinone which were recrystallized from ethanol (200 proof) prior to use. SERRS experiments involving hypericin were carried out using a solution of hypericin (approximately 10^{-5} M) in DMSO (Fisher Scientific, Fair Lawn, NJ) , DMSO in chloroform or ethanol. The DMSO was dried over molecular sieves (3 Å) to remove residual water. The chloroform was HPLC grade (Fisher Scientific, Fair Lawn, NJ) and was used without further purification. For SERS, the model compounds were dissolved in benzene (HPLC Grade, Omnisolve EM Science) prior to adsorption from the solution onto the SERS substrate..

The absorption spectra of hypericin and its model compounds were obtained with a Perkin Elmer Lambda 6 spectrophotometer. Scan rate = 600 nm/min, slit width = 1 nm, path length = 1 cm. Spectra of the model compounds were obtained from benzene solutions.

Fluorescence spectra for hypericin were determined using an Aminco SLM 8000 spectrofluorometer. The excitation wavelength was 550 nm and the emission was monitored between 590 and 850 nm. The fluorescence spectra were detected perpendicular to the beam from the excitation source. The resolution of the excitation and emission monochrometers was 4 nm. Absorption and fluorescence spectra were obtained at room temperature.

SERRS spectra for all compounds were obtained from an electrochemically roughened Ag electrode as the SERRS substrate. The

electrode was dipped into a solution of the appropriate compound for approximately 15 minutes, removed from the solution and placed, without rinsing, in a liquid nitrogen optical dewar. The scattered radiation was collected in a backscattering geometry. Hypericin SERRS spectra were taken with several excitation wavelengths: 406.7, 457.8, 488.0 and 514.5 nm. A Coherent Innova Kr^+ 100 (406.7 nm) and Ar^+ 200 series (457.8, 488.0, 514.5 nm) laser was used as the excitation source. The laser power at the sample was approximately 20 mW and the integration time was 20 sec. SERS spectra of the model compounds were obtained using 488.0 nm excitation. SERRS spectra for all compounds were compared at this wavelength.

Raman spectra of the analogs and RR spectra of hypericin were obtained from solid samples packed in capillary tubes. Hypericin spectra were obtained at 457.8, 488.0 and 514.5 nm. Raman spectra of the model compounds were acquired using 488.0 and 514.5 nm excitation. Spectra for all compounds were compared at 488.0 nm. All spectra of solid samples were taken at room temperature.

Spectra at all excitation wavelengths except 406.7 nm were recorded using a Spex Triplemate spectrometer with a Princeton Applied Research Corp. (PARC) intensified SiPD detector (model 1421–R–1024HD) cooled to –40 C. For detection at 406.7 nm, a Spex Triplemate spectrometer with a PARC model 1420 detector was used. This detector was tap water cooled. All spectra were plotted using Spectra Calc (Galactic Software, Salem, NH) and were baseline corrected and smoothed.

RESULTS

The absorption and fluorescence spectra (Figs. 3a and 3b) of hypericin obtained in DMSO are similar to those previously reported for ethanol solutions with respect to peak position and shape (Scheibe and Schontag, 19421; Walker *et al.*, 1979; Jardon and Gautron, 1989). Pace and Mackinney (1939) described the effect of solvent on the absorption spectrum of hypericin in the visible region (450 to 600 nm). DMSO was not used in their study. Table I compares the positions of the major absorption and emission bands in DMSO to those in other solvents. The extinction coefficient in DMSO was determined to be 43,000. This is very close to the value of 41,600 (in ethanol) reported by Scheibe and Schontag (1942). Serial dilutions (spectra not shown) were performed in an effort to asses the amount of aggregation present in both DMSO and ethanol. No change was observed in the ethanol spectrum on decreasing the concentration from 4×10^{-4} M to 4×10^{-8} M. Some differences were present in the absorption spectrum of hypericin in DMSO at low concentration (10^{-8} M) compared to 10^{-4} M. These results suggest that the hypericin is monomeric in polar solvents between 10^{-6} and 10^{-4} M. In non-polar solvents, chloroform/hexane (8:2 v/v), there are small differences in the peak positions compared to those in polar solvents. Our results are in agreement with those published by Pace and MacKinney (1939).

The fluorescence spectrum was affected in a manner similar to that of the absorption spectra. The emission maxima are blue shifted by approximately 10 nm in ethanol compared to those in DMSO.

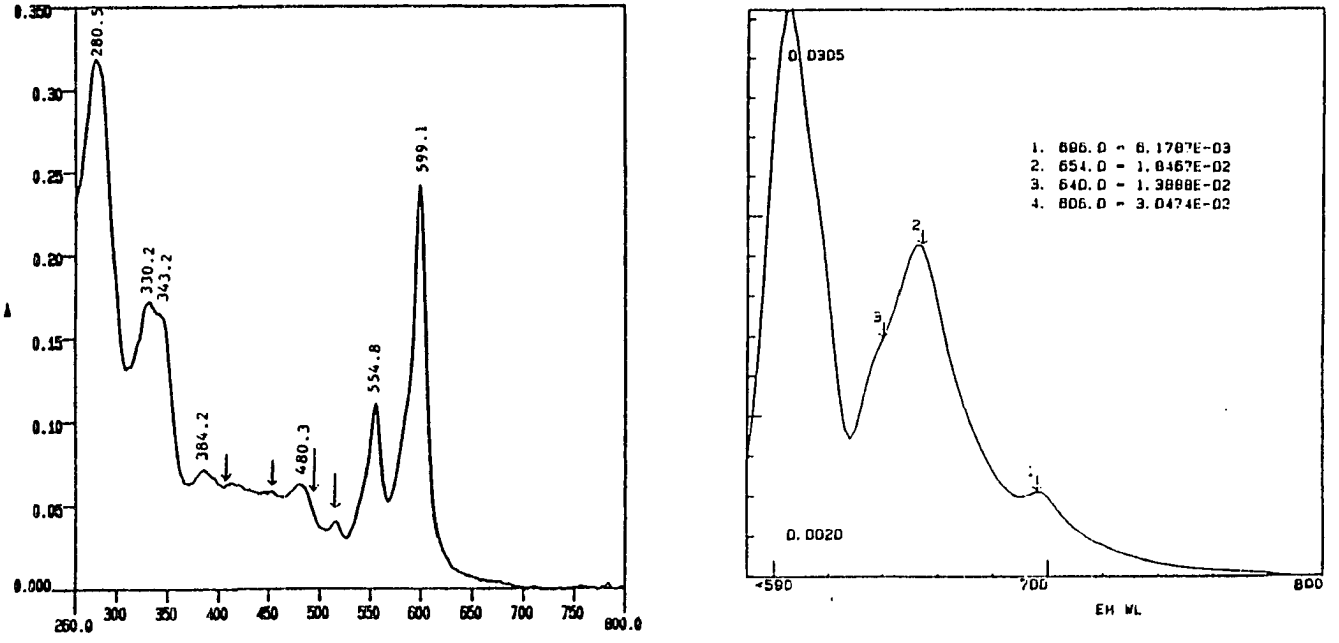

Figure 3. a) Absorption spectrum of hypericin in DMSO (approx. 10^{-} M). Raman excitation wavelengths are marked by arrows. b) Fluorescence spectrum of hypericin in DMSO

Table 1. Absorption and emission maxima for hypericin in various solvents

Solvent	Absorption Maxima (nm)									Emission Maxima (nm)		
DMSO	599		555	514	480	384	343	333	281	708	654	606
Aq. DMSO	597	581	554	516	481	386	342	332				
Ethanol	591	578	547	510	477	383	337	326	284	699	644	597
Acetone*	596		551	514	477					700	649	601
Chloroform/ hexane (8:2)	601		563	525	489	388		332				
Pyridine*	603		558	520	483							

*Absorption data taken from Pace and Mackinney (1939).

The excitation wavelengths used for RR and SERRS are indicated by the arrows on the absorption spectrum in Figure 3a. The extinction coefficients for these transitions are relatively low but are still sufficient to obtain large resonant enhancement. Excitation wavelengths closer to the more intense optical transitions could not be used. At 568 nm, the fluorescent background completely overwhelmed the Raman spectrum and at 351.0 nm surface enhancement is negligible. Attempts to measure resonance Raman spectra in DMSO solution at several wavelengths were unsuccessful due to the large fluorescence background. However, RR spectra were obtained from the solid sample.

The RR and SERRS spectra of hypericin are shown in Figures. 4 and 5. Table II compares the peak positions in the high frequency region for the two methods. The spectra are very similar at each excitation wavelength. Some minor frequency shifts occur with adsorption of the hypericin onto the roughened silver substrate and there are also some differences in band intensities between the two sets of spectra. However, the similarity between the spectra indicate the absence of strong chemical interactions between the Ag surface and hypericin.

The carbonyl bands, normally present between 1660 to 1700 cm^{-1}, are not visible in either the SERRS or RR spectra of hypericin. The SERRS effect produces the largest enhancement of vibrational modes which have their transitions perpendicular to the surface. Absence of the carbonyl bands in the SERRS spectra suggests two possibilities: 1) the hypericin adsorbs through one carbonyl group but the excitation wavelengths used are not in resonance with a transition dipole being along the axis of the carbonyl group or 2) the

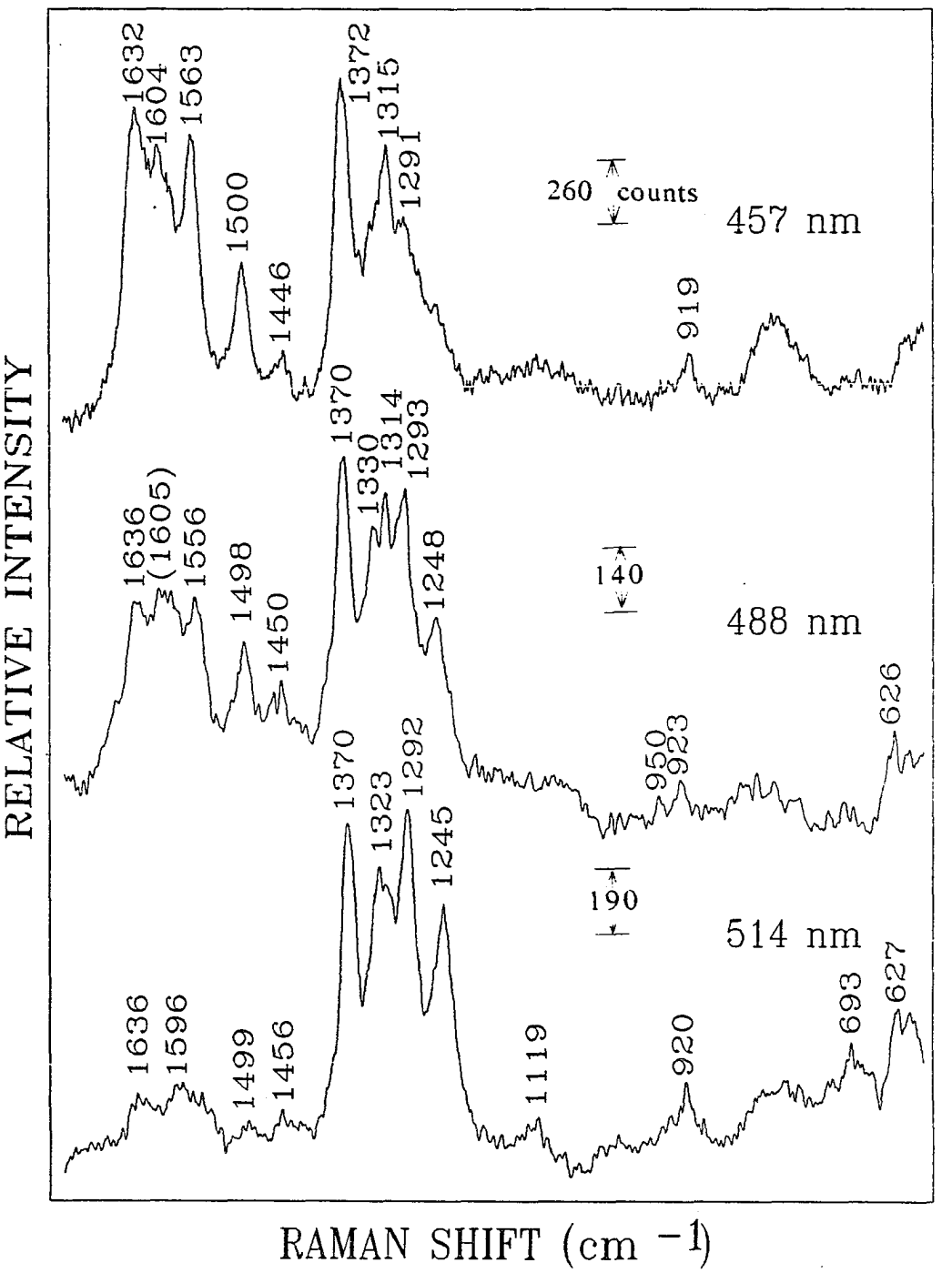

Figure 4. Resonance Raman spectra of solid hypericin. a) 457.9 nm, b) 488.0 nm, c) 514.5 nm. Integration time, 20 seconds; laser power, 20 mW; spectral resolution, 4 cm^{-1}

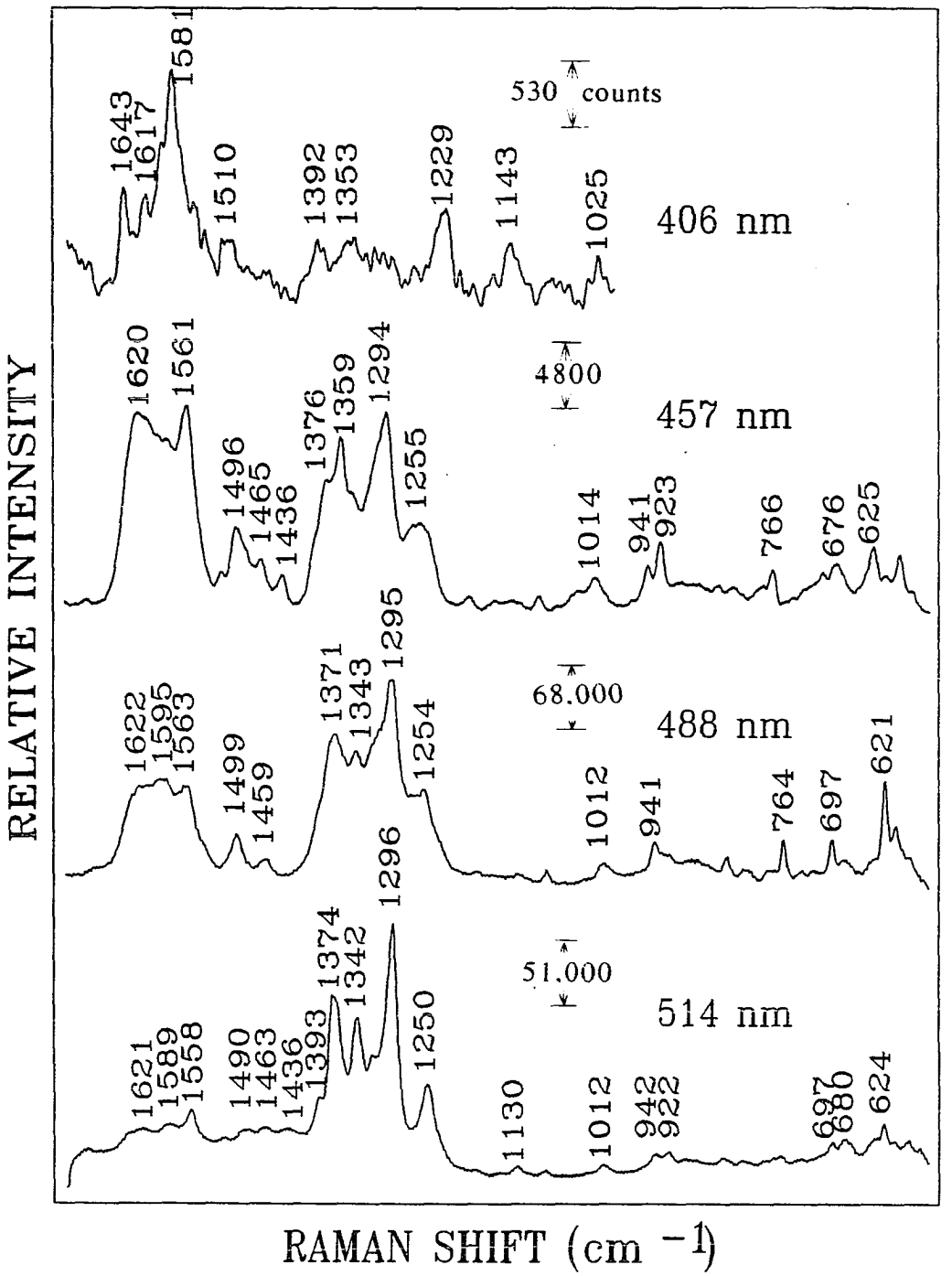

Figure 5. SERRS spectra of hypericin. a) 406.7 nm, b) 457.9 nm, c) 488.0 nm, d) 514.5 nm.

Table 2. Hypericin RR and SERRS at different wavelengths.

406.7 nm	457.9 nm		488.0 nm		514.0 nm	
SERRS	RR	SERRS	RR	SERRS	RR	SERRS
1643						
1617	1632	1620	1636	1622	1636	1621
1581	1604		(1605)	1595	1596	1589
	1563	1561	1556	1563		1558
(1510)	1500	1496	1498	1499	1499	1490
	1446	1465	1450	1459	1456	1463
		1436				1436
1392						1393
	1372	1376	1370	1371	1370	1374
1353		1359				
			1330	1343	1323	1342
	1315		1314			
	1292	1294	1293	1295	1292	1296
		1255	1248	1254	1245	1250
1229						
1143					1119	1130
1025		1014		1012		1012
		941	950	941		942
	919	923	923		920	922

hypericin adsorbs to the surface in a different orientation e.g. the four hydroxy groups are closest to the surface and the carbonyl groups are parallel. Langmuir–Blodgett (L.-B.) monolayer studies of hypericin (to be published) have indicated an area of approximately 55 Å per hypericin molecule. SERRS spectra of hypericin adsorbed from a L.-B. monolayer are similar to those formed from self-adsorption. This implies the hypericin adsorbs in the same manner using these two methods. The observed area is smaller than the calculated area of hypericin if the rings are parallel to the surface. Therefore, the hypericin may be adsorbing at some angle relative to the surface or the molecules may form stacks.

Preliminary results suggest that the first hypothesis is the correct one. This is based on the observation of a strong band at 1643 cm^{-1} with 406.7 nm excitation. The band is somewhat low for a C=O stretch but this may be due to conjugation with the hydroxy groups. No RR spectrum of the solid was obtained at this wavelength.

The most pronounced difference between the RR and SERRS spectra is the considerable enhancement of the 1370 cm^{-1} band at all excitation wavelengths in the RR spectra. This intensity difference is much less pronounced at 514.5 nm. The 1370 cm^{-1} band has been tentatively assigned to an in–plane vibration of the central fragment, the portion of the molecule containing the carbonyl groups (rings II and VII). This assignment is based on comparison with PQ spectra (Gastilovich *et al.*, 1986). Other differences include an increase in intensity of the band at approximately 1315 cm^{-1} with 488.0 and 514.5 nm excitation and the disappearance of the band at 1359 cm^{-1} in the RR vs SERRS spectrum taken at 457.8 nm. Both vibrational bands fall

in the region of CC in-plane stretching modes (Abasbegovic *et al.*, 1964; Dollish *et al.*, 1964).

To assign the Raman bands of hypericin, Raman and SERS spectra of the model compounds were determined. Raman spectra of anthracene (A) and anthraquinone (AQ) have been reported in the literature (Abasbegovic *et al.*, 1964; Netto *et al.*, 1966; Singh and Singh, 1968; Stenmann, 1969; Lehmann *et al.*, 1979; Gastilovich *et al.*, 1986; Dutta and Hutt, 1987). The bands observed here agree with those reported previously. Spectra were obtained at two wavelengths, 488.0 and 514.5 nm, in an effort to circumvent the fluorescence associated with several of the compounds. These spectra are shown in Figs. 6 and 7. The anthracene spectrum was superimposed on the very high fluorescence background at 488.0 nm. This background was much less with excitation at 514.5 nm. Anthraquinone spectra showed little interference from fluorescence at either wavelength but the spectrum was more intense with 488.0 nm excitation. The Raman spectra for the analogs anthraflavin (AF), 9,10-phenanthrenequinone (PQ) and emodin (E) had very high backgrounds and low signal to noise ratios and some Raman bands were difficult to distinguish. No bands were visible in the spectrum of AF acquired with 514.5 nm excitation. Spectra for the analogs are very similar at both wavelengths. Some minor differences were observed between the emodin spectra but this is due to a resonance enhancement of certain modes with excitation at 488.0 nm. From the absorption spectrum of emodin (not shown) it can be seen that the resonance effect should be much weaker at 514.5 nm.

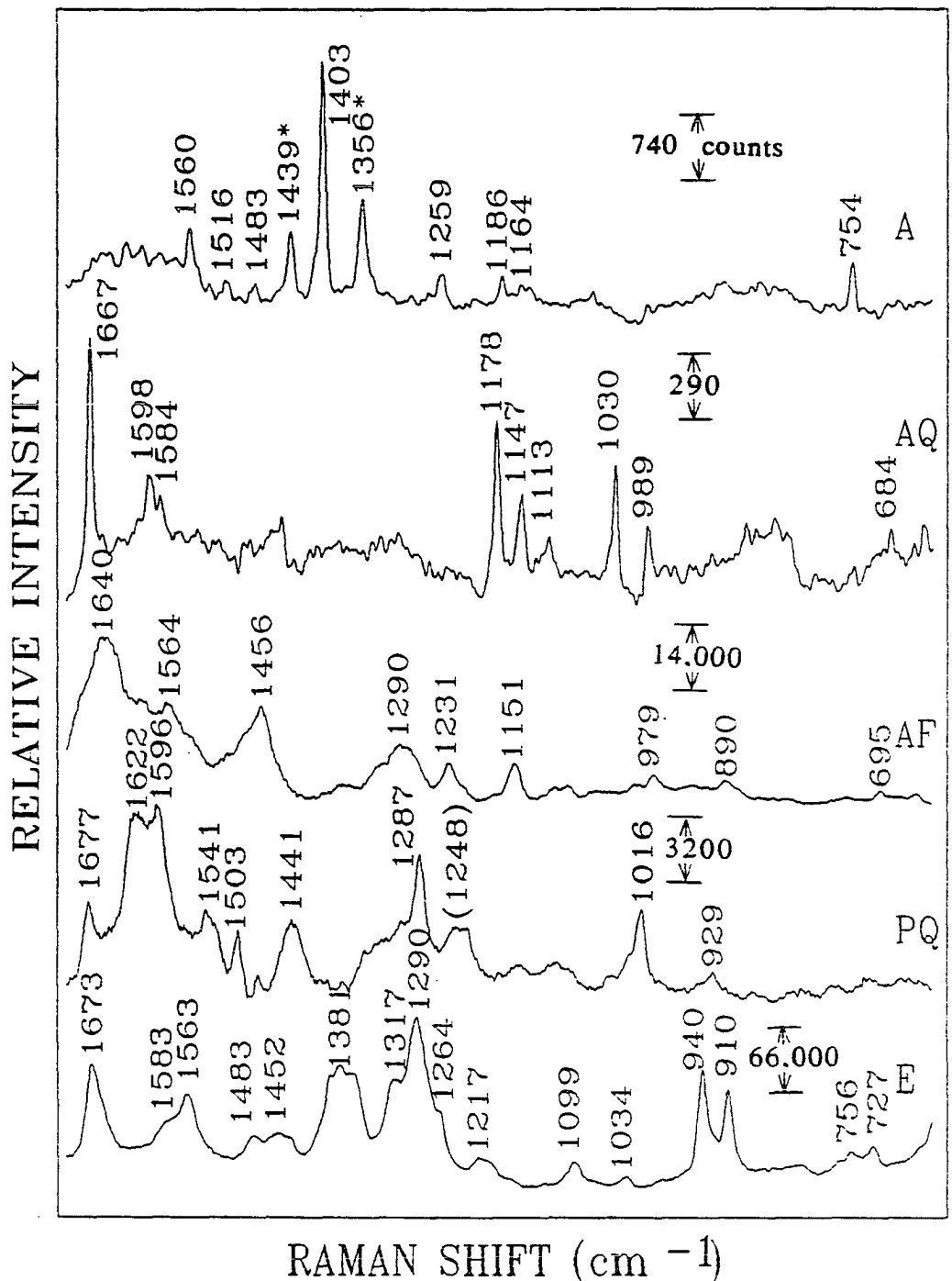

Figure 6. SERS spectra of A, AQ, AF, PQ, and E with 488.0 nm excitation

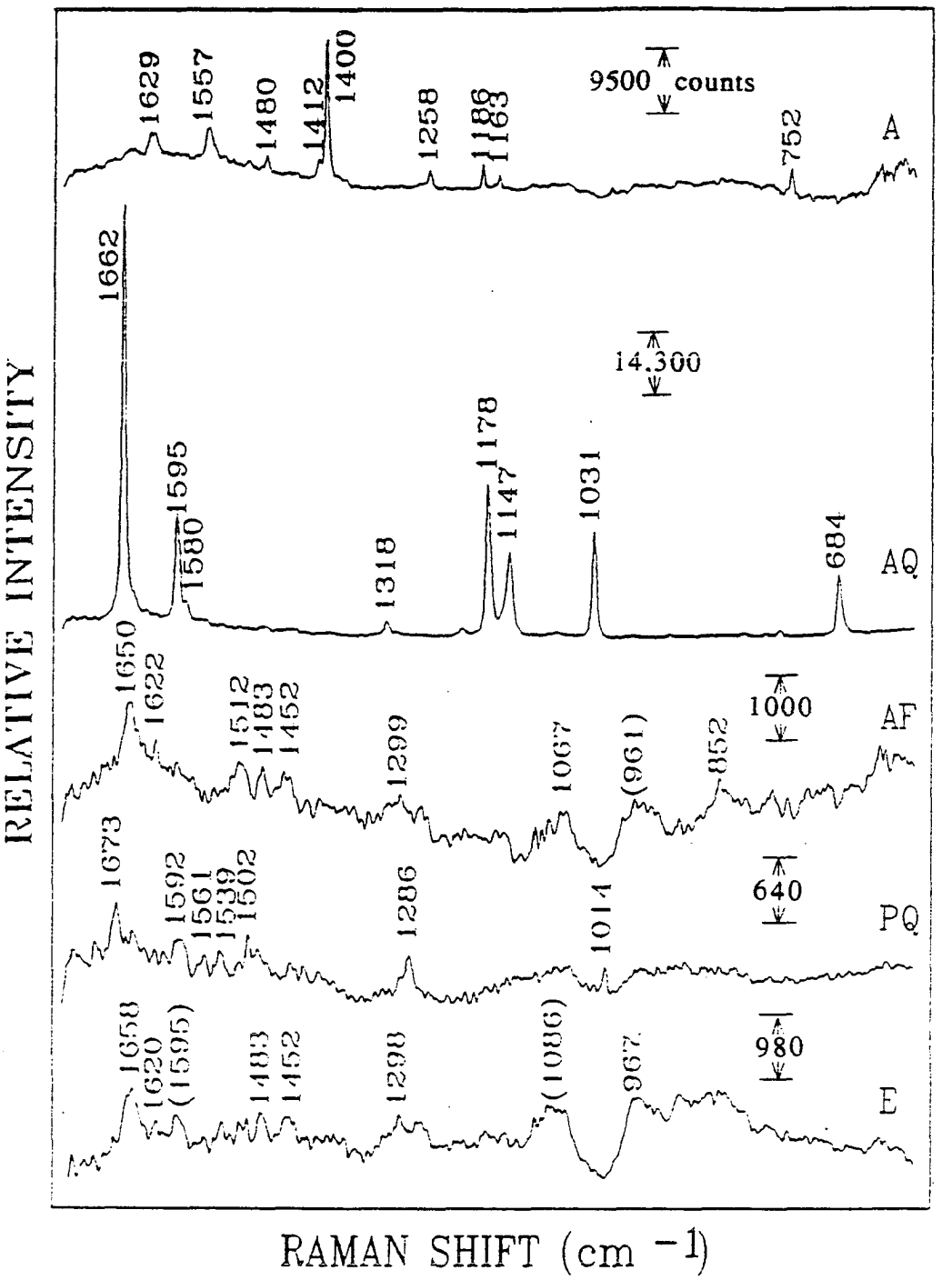

Figure 7. Raman spectra of A, AQ, AF, PQ, and E solids with 488.0 nm excitation

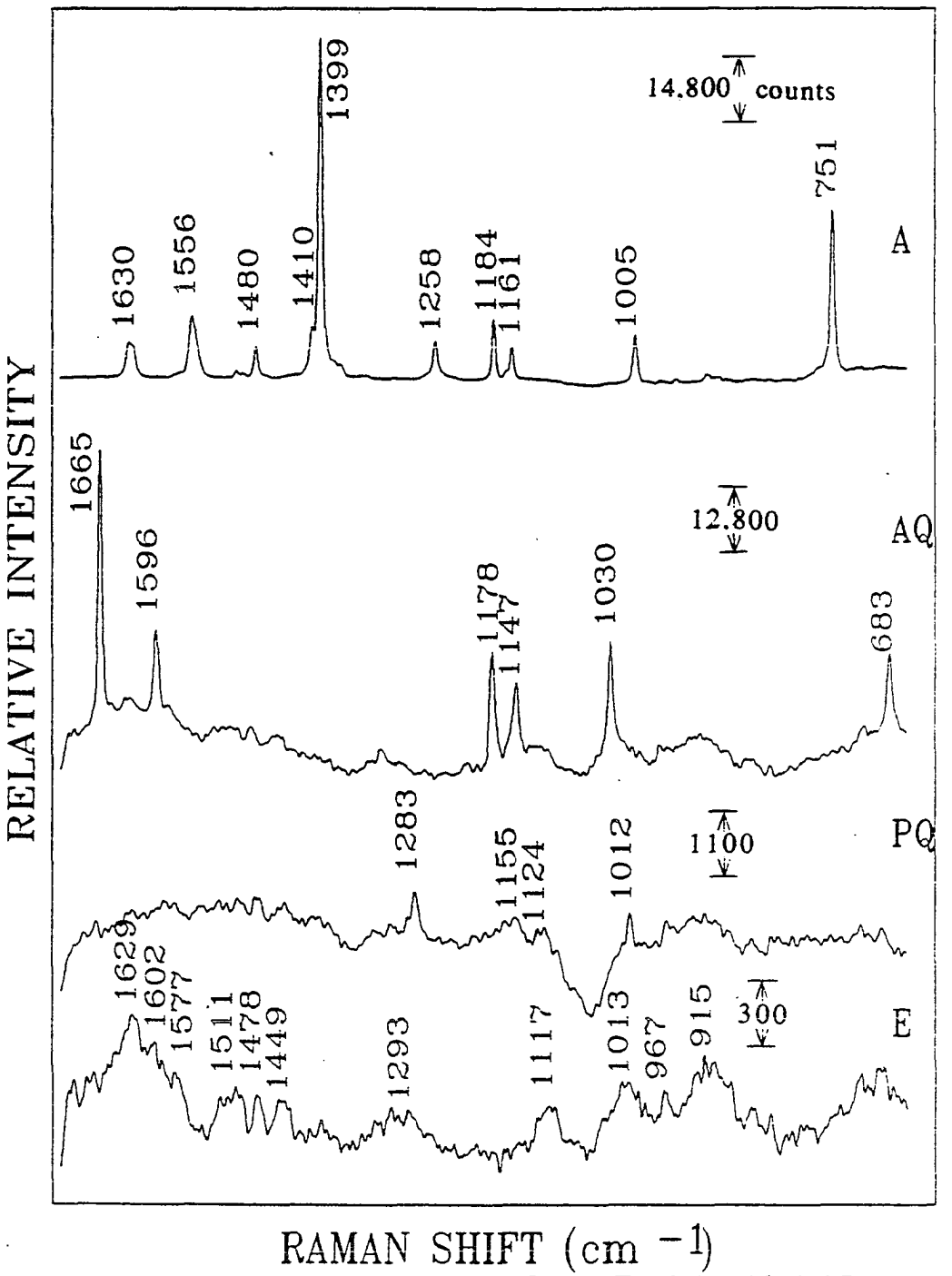

Figure 8. Raman spectra of A, AQ, AF, PQ, and E solids with 514.5 nm excitation

Table 3. Raman (488.0 nm and 514.0 nm) and SERS (488.0 nm) bands for model compounds

A			AQ			AF		PQ			E		
Raman		SERS	Raman		SERS	Raman	SERS	Raman		SERS	Raman		SERS
514 nm	488 nm	488 nm	514 nm	488 nm	488 nm	488 nm	488 nm	514 nm	488 nm	488 nm	514 nm	488 nm	488 nm
			1665	1662	1667				1673	1677		1658	1673
						1650	1640						
1630	1629					1622				1622	1629	(1620)	
			1596	1595	1598				1592	1596	1602	(1595)	
				1580	1584								1583
1556	1557	1560					1564		1561		1577		1565
									1539	1541			
		1516				1512			1502	1503	(1511)		
1480	1480	1483				1483					1478	1483	1483
						1452	1456				1449	1452	1452
		1439*								1441			
1410	1412												
1399	1400	1403											1381
		1356*											
													1317
				1316									
						(1299)	1290	1283	1286	1287	1293	1298	1290
1258	1258	1259					1231			(1248)			1264
1184	1186	1186	1178	1178	1178								
1161	1163	1164	1147	1147	1147		1151	1155					
					1113			(1124)			1117		
												(1086)	1099
						1067							
			1030	1031	1030								1034
1005								1012	1014	1016	1013		
					989		979						
						(961)					967	(967)	940
										929	915		910
						852							
													756
751	752	754											727
			683	684	684		695						

SERS spectra of the of anthracene and anthraquinone at 488.0 nm showed much lower signal to noise ratios compared to the Raman spectra on the solid samples. There are several possibilities as to why this is the case. First, these compounds have a low solubility in benzene. This may have resulted in less than a monolayer of coverage in the adsorption step. Second, these compounds may not adsorb strongly to the metal surface. Fluorescence was still present but was significantly quenched so that the spectra of AF, PQ and E were observed. Table III compares the Raman and SERS bands observed for the model compounds.

The vibrational bands and general assignments for hypericin and the model compounds are listed in Table 4. The bands listed for hypericin are a compilation of bands observed at all wavelengths. It should be noted that there is some disagreement in the literature regarding the exact vibrational assignments for these compounds hence the assignments proposed here are tentative (Abasbegovic *et al.*, 1964; Dollish *et al.*, 1964).

The hypericin SERRS spectrum is most similar to the spectra of AF, E and PQ. The similarity to PQ was unexpected because, at first glance, the structure of hypericin can be thought of as two fused anthraquinones. This conclusion is supported by similarities with the spectra of AF and E, both modified anthraquinones. Based on the vibrational spectrum, however, it also appears that the hypericin structure can be viewed as four interconnecting PQ structures, with each carbonyl fragment common to two PQ structures (see dashed line in Fig. 1). Close proximity of oxygen atoms, whether as carbonyl or hydroxy groups, may also account for the similarity in

Table 4. Comparison of hypericin and model compound SER(R)S spectra with 488.0 nm excitation

A	AQ	AF	PQ	E	Hyp	Assignment[a]
	1667		1677	1673		C=O
	1650	1640			1643	CC in-plane
			1622		1620	stretch
	1598		1596			
	1584			1583	(1587)	
1560		1564		1564	1559	
			1541			
1516						
			1503		1500	
1483				1483		
		1456		1452	1460	
1439*			1441		1436	
1403				1381	1393	
					1374	
1356*					1356	
					1342	
				1317		
		1290	1287	1290	1295	
1259			(1248)	1264	1251	
		1231			1229	
1186	1178					CH in-plane
1164	1147	1151			1143	bend
	1113			1099		
	1030			1034		
			1016		(1015)	CC in-plane
	989	979				bend
				940	941	
			929	910	920	

[a]Assignments are taken from Abasbegovic et al, 1964; Dollish et al. 1964; Lehmann et al, 1979; and Dutta and Hutt, 1987.

*These bands were only visible in the SERS spectrum. The cause of these bands is unknown.

Bands in parentheses are an average value.

features between AF, E, PQ and hypericin. These interactions would be impossible in AQ but not in the other model compounds.

Carbonyl bands are found in the region of 1660 to 1700 cm^{-1}. The carbonyl band for E is very pronounced in the SERS spectrum while it is weak in the spectrum of the solid. This indicates that E adsorbs perpendicularly to the surface, perhaps through one of the carbonyl groups. The carbonyl bands in PQ are not as pronounced as in E. However, the bands in this region of the PQ spectrum are not well resolved which may partially account for this observation.

Because of uncertainty of assignments in the model compounds, the hypericin bands cannot be assigned in an unambiguous manner. Bands in the region of 1650 to 1230 cm^{-1} are assigned as CC stretching vibrations, most likely due to the outer benzene fragments or the four "corner" rings (see Fig.1) (Gastilovich *et al.*,, 1986). The band at 1331 cm^{-1} by comparison to PQ and AQ is a CC in–plane bending vibration of the outer benzene fragments and the 1370 cm^{-1} band is due to in–plane vibrations of the central fragment , the portion of the molecule containing the carbonyl group (Gastilovich *et al.*, 1986). Bands between 1160 to 1100 cm^{-1} are from CCH in–plane bending modes and bands in the region from 1030 to 680 cm^{-1} are due to CC in–plane bending vibrations (Abasbegovic *et al.*, 1964; Dollish *et al.*, 1964; Lehmann *et al.*, 1979; Dutta and Hutt, 1987)

The hypericin spectrum does not closely resemble either anthracene or AQ although there are several bands in common. In particular, the bands assigned to CC in-plane stretch and a strong band at approximately 750 cm^{-1} assigned to a CC in-plane bending vibration.

Hypericin has C_{2v} symmetry and has 152 normal modes distributed between four symmetry species, A_1, A_2, B_1 and B_2. All modes are Raman and IR allowed except for the A_2 modes which are IR forbidden. Infrared studies involving hypericin are therefore necessary to assist in the assignments of the vibrational bands.

CONCLUSIONS

The RR and SERRS spectra of hypericin show a great deal of similarity, indicating a weak interaction between the hypericin and the Ag substrate. This was also observed in the case of the model compounds, especially A and AQ. High quality spectra were obtained using this technique. In addition, fluorescence was quenched by the SERS substrate allowing spectra of AF, PQ and E to be obtained. Because of these two factors, SERRS should prove useful as a sensitive technique for the study of hypericin containing systems, e.g. study of model membrane systems or native systems (viruses).

Due to the complexity of the hypericin structure and, hence, the vibrational spectrum, exact assignments of vibrational bands are not possible without a normal mode analysis. Further experiments are necessary before more exact assignment are justified. These experiments should include the use of IR spectroscopy, different model compounds and isotopic substitution. To facilitate the assignments of the vibrational spectrum, identification of the electronic transitions giving rise to the absorption spectrum would also be useful.

The fact that the hypericin spectrum more closely resembles PQ than AQ is somewhat surprising. The Raman results may indicate a conjugation pathway in hypericin that is similar to that found in 9,10-phenanthrenequinone.

ACKNOWLEDGEMENT

This work was supported by a Biotechnology grant from Iowa State University.

REFERENCES

Abasbegovic N., N. Vukotic and L. Colombo (1964) Raman spectrum of anthracene. *J. Chem. Phys.* 41, 2575-2577.

Brockmann, H. H. (1952) Photodynamically active natural pigments. *Prog. Org. Chem.* 1, 64-82.

Blum, H. F. (1941) *Photodynamic Action and Diseases Caused by Light.* Reinhold, New York.

Carpenter, S. and G. A. Kraus (1991) Photosensitization is required for inactivation of Equine Infectious Anemia Virus by hypericin. *Photochem. Photobiol.* 53, 169-174.

Cotton, T. M. (1988) The application of surface-enhanced Raman scattering to biochemical systems. in *Spectroscopy of Surfaces, Vol. 16.* (Edited by R. J. H. Clark and R. E. Hester), pp 91-153. John Wiley & Sons, New York.

Dollish, F. R., W. G. Fateley and F. F. Bentley (1974) *Characteristic Raman Frequencies of Organic Compounds.* John Wiley & Sons, New York.

Duran, N. and P.-S. Song (1986) Hypericin and its photodynamic action. *Photochem. Photobiol.* 43, 677-680.

Dutta, P. K. and J. A. Hutt (1987) Infrared and resonance Raman spectroscopic studies of 1-hydroxy-9,10-anthraquinone and its metal complexes. *J. Raman Spectros.* 18, 339-344.

Gastilovich, E. A., V. G. Klimenko, T. S. Kopteva, I. A. Migel' and D. N. Shigorin (1986) Detailed interpretation of the vibrations of polyatomic molecules with a low-symmetry nuclear configuration. *Russ. J. Phys. Chem.* (Eng. trans.) 60, 69-73.

Giese, A. C. (1971) Photosensitization by natural pigments. *Photophysiology.* 6, 77-129.

Giese, A. C. (1980) Hypericism. *Photochem. Photobiol. Rev.* 5, 229-255.

Hudson, J. B., I. Lopez-Bazzocchi and G. H. N. Towers (1991) Antiviral activities of hypericin. *Antiviral Res.* 15, 101-112.

Ito, T. (1978) Cellular and subcellular mechanisms of photodynamic action: The $^1O_2$ hypothesis as a driving force in recent research. *Photochem. Photobiol.* 28, 493-508.

Jardon, P., N. Lazorchak and R. Gautron (1986) Propriétés du premier état triplet de l'hypericine étude par spectroscopie laser. *J. Chim. Phys. Phys.-Chim. Biol.* 83, 311-315.

Jardon, P., N. Lazorchak and R. Gautron (1987) Formation d'oxygene singulet $^1\Delta_g$ photosensibilisée par l'hypericine. Charactérisation et étude du mécanisme par spectroscopie laser. *J. Chim. Phys. Phys.-Chim. Biol.* 84, 1141-1145.

Jardon P. and R. Gautron (1989) Photophysical properties of hypericin in solution and in micellar dispersion. *J. Chim. Phys. Phys.-Chim. Biol.* 86, 2173-2190.

Knox, J. P., R. I. Samuels, and A. D. Dodge (1987) Photodynamic action of hypericin. in *Light Activated Pesticides*, (Edited by J. R. Heitz and K. R. Downum), pp 265-270. Washington, DC: American Chemical Society.

Knox, J. P. and A. D. Dodge (1985) Isolation of the photodynamic pigment hypericin. *Plant, Cell Environ.* 8, 19-25.

Lehmann, K. K., J. Smolarek, O. S. Khalil and L. Goodman (1979) Vibrational spectra of anthraquinone. *J. Phys. Chem.* 83, 1200-1205.

Lopez-Bazzocchi, I., J. B. Hudson and G. H. N. Towers (1991) Antiviral activity of the photoactive plant pigment hypericin. *Photochem. Photobiol.* 54, 95-98.

Neto, N., M. Scrocco and S. Califano (1966) A simplified valence force field of aromatic hydrocarbons-I Normal coordinate calculations for C_6H_6, C_6D_6, $C_{10}H_8$, $C_{10}D_8$, $C_{14}H_{10}$ and $C_{14}D_{10}$. *Spectrochim. Acta.* 22, 1981-1998.

Pace. N. (1942) The eitology of hypericism, a photosensitivity produced by St. Johns-wort. *Am. J. Physiol.* 136, 650-656.

Pace, N. and G. Mackinney (1939) On the absorption spectrum of hypericin. *J. Am. Chem. Soc.* 61, 3594-3595.

Pace, N. and G. Mackinney (1941) Hypericin, the photodynamic pigment from St. Johns-wort. *J. Am. Chem. Soc.* 63, 2570-2574.

Racinet, H., P. Jardon, R. Gautron (1988) Formation d'oxygégen singulet $^1\Delta_g$ photosensibilisée par l'hypericine étude cinétique en milieu micellaire non ionique. *J. Chim. Phys. Phys.-Chim. Biol.* **85**, 971-977.

Scheibe, G. and A. Schontag (1942) Lichtabsorption und Fluorescnz des Hypericins. *Chem. Ber.* **75**, 2019-2026.

Singh, S. N. and R. S. Singh (1968) Vibrational spectra of condensed ring quinones-I 1,4-naphthoquinone and 9,10-anthraquinone. *Spectrochim. Acta.* **24A**, 1591-1597.

Song, P.-S., D.-P. Hader and K. L. Poff (1980) Phototactic orientation by the ciliate, *Stentor coeruleus. Photochem. Photobiol.* **32**, 781-786.

Stenman, F. (1969) Raman scattering from powdered 9,10-anthraquinone. *J. Chem. Phys.* **51**, 3413-3414.

Thomson, R. H. (1971) *Naturally Occurring Quinones.* Academic Press, New York.

Turro, N. J. (1978) *Modern Molecular Photochemistry.* The Benjamin/Cummings Publishing Co., Inc., Reading, MA.

Walker, E. B., T. Y. Lee and P.-S. Song (1979) Spectroscopic characterization of the stentor photoreceptor. *Biochim. Biophys. Acta.* **587**, 129-144.

Yang, K.-C., R. K. Prusti, E. B. Walker, P.-S. Song, M. Watanabe and M. Furuya (1986) Photodynamic action in *Stentor coeruleus* sensitized by endogenous pigment stentorin. *Photochem. Photobiol.* **43**, 305-310.

SECTION IV. PHOTODYNAMIC ACTION SPECTRUM OF HYPERICIN AND LOCALIZATION OF HYPERICIN IN THE VIRUS BY SURFACE ENHANCED RESONANCE RAMAN SCATTERING SPECTROSCOPY

INTRODUCTION

Hypericin, Figure 1, is a fluorescent photodynamic pigment found in certain varieties of the *Hypericum* genus. On exposure to light, hypericin can act as a sensitizer. It causes a disease called hypericism that manifests itself in severe photosensitivity in grazing animals that have ingested hypericin containing plants. In extreme cases it may lead to the death.[1-5] Hypericin has other effects as well. It has been used as an antidepressant[4] and was recently shown to be efficacious against certain retroviruses including equine infectious annemia virus (EIAV)[7], murine cytomegalovirus (MCMV), sindbus virus (SV)[8,9], and HIV[10,11]. Hypericin's photodynamic effects are thought to be the result of one of two mechanisms; Type I which leads to the formation of radicals or Type II in which singlet oxygen is formed. In vitro experiments have shown that hypericin can function by both mechanisms,[12-14] but based on studies involving structurally similar compounds, it is believed that the Type II mechanism is predominant.[15]

This study was designed to 1) assess the action spectrum of hypericin for photodestruction of EIAV and 2) determine the interaction and environment of hypericin with respect to the EIAV using surface enhanced resonance Raman scattering (SERRS) spectroscopy. The second goal should provide information regarding the mode of action of hypericin for viral inactivation in addition to determining whether the hypericin is loosely associated with the virus,

tightly bound to the virus surface or is incorporated into the virus particle itself.

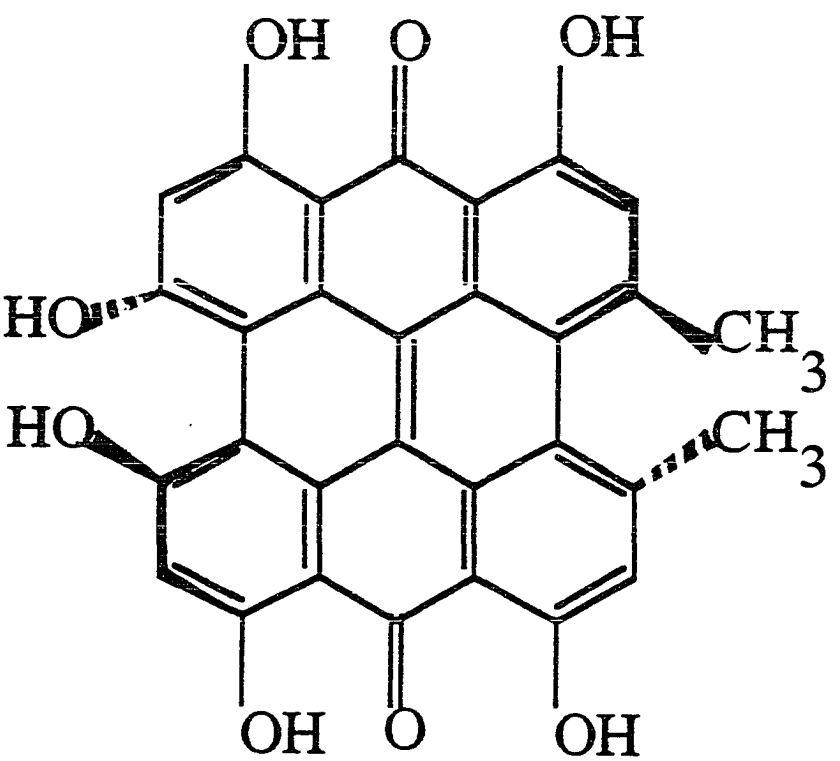

Figure 1. Structure of hypericin

MATERIALS AND METHODS

Hypericin was synthesized and purified in Dr. G. Kraus' laboratory at Iowa State University, Ames, IA. Equine infectious annemia virus (EIAV) was obtained from Dr. S. Carpenter at Iowa State University. Spectroscopic experiments to determine the action spectrum of hypericin were performed on a SLM–Aminco 8000 spectrofluorometer. Wavelengths corresponding to several absorption maxima in hypericin (350, 450, 550, 600, and 700 nm) were used. Entrance slits to the sample compartment were set for maximum illumination of the sample. Exposure time at each wavelength was 20 min. Relative intensities of the incident radiation was measured by a photovoltaic cell.

One milliliter volumes containing approximately 10^3 focus forming units (FFU) of EIAV in TNE and 10 μg/ml hypericin in DMSO were placed in a microcuvette and illuminated for 20 minutes at the aforementioned wavelengths. A blank of virus and DMSO were also analyzed at each wavelength as an internal control. Additional controls included the use of white light and no light for the same amount of time. After light exposure, the virus was diluted with Polybrene (8 mg/ml) inoculated into equine dermal (ED) cells, which had been seeded the previous day in 60 mm tissue culture dished at a concentration of 2×10^5 cells per dish. Five days later, the cells were fixed in 100% methanol and tested for the presence of EIAV using indirect immunofluorescence. Foci of EIAV–infected cells were counted. To compensate for any antiviral effects due to excitation

wavelengths, results are expressed as the percent reduction of foci in hypericin treated samples as compared to control samples at the same wavelength.

Four samples were examined by SERRS spectroscopy. 1) MDBK (virus negative cell cultures), 2) MDBK with hypericin, 3) WYO (a strain of EIAV), and 4) WYO with hypericin. For concentration and purification of virus, supernatent was collected from EIAV–infected cells, clarified by centrifugation and polyethylene glycol (PEG–8000) was added to a final concentration of 6% PEG. Virus was precipitated by centrifugation at 10,000 x g for 30 min and the precipitate was dissolved in TNE (10 mM Tris–HCl, pH 7.4, 150 mM NaCl, 1 mM EDTA) containing 1 mM PMSF. Concentrated virus was layered on a discontinuous sucrose gradient (15%/65%) in TNE and centrifuged at 10,000 x g for 60 min. Virus collected from the interface was dialyzed to remove sucrose.

Two mg EIAV in 2.0 ml TNE were added to hypericin to a final concentration of 10 μg/ml hypericin in TNE. The mixture was overlaid onto a discontinuous sucrose gradient, centrifuged, and EIAV was purified from the interface as before. Control samples included purified virus without hypericin as well as hypericin–treated and control samples prepared from virus–negative cell cultures (MDBK). In the case of MBDK with hypericin, the hypericin remained at the interface. The virus with hypericin sample, however,contained most of the hypericin in the pellet at the bottom of the centrifuge tube while only a small portion remained associated with the virus. Samples

were not dialyzed prior to spectroscopic analysis in an effort to keep the samples as concentrated as possible.

SERRS spectra were obtained from each of the four samples. A silver colloid with λ_{max} = 410 nm was used as the SERRS substrate. The scattered radiation was collected in a backscattering geometry. SERRS spectra were taken with 488.0 nm excitation from a Coherent Innova Ar^+ 200 series laser. Spectra were recorded using a Spex Triplemate spectrometer with a Princeton Applied Research Corp. (PARC) intensified SiPD detector (model 1421–R–1024HD) cooled to –40 C. All spectra were baseline and background corrected and were plotted using spectra Calc (Galactic Software, Salem, NH).

RESULTS

Pace (1942)[16] reported that the action spectrum for hypericin induced photosensitivity in rabbits sensitized by a hypericin diet, was similar to the absorption spectrum. The greatest amount of photosensitization occurred at wavelengths corresponding to the red-most absorption bands at 550 and 600 nm. Wavelengths longer than 610 nm had little effect. The absorption spectrum of hypericin is displayed in Figure 2. The spectrum is identical to previously

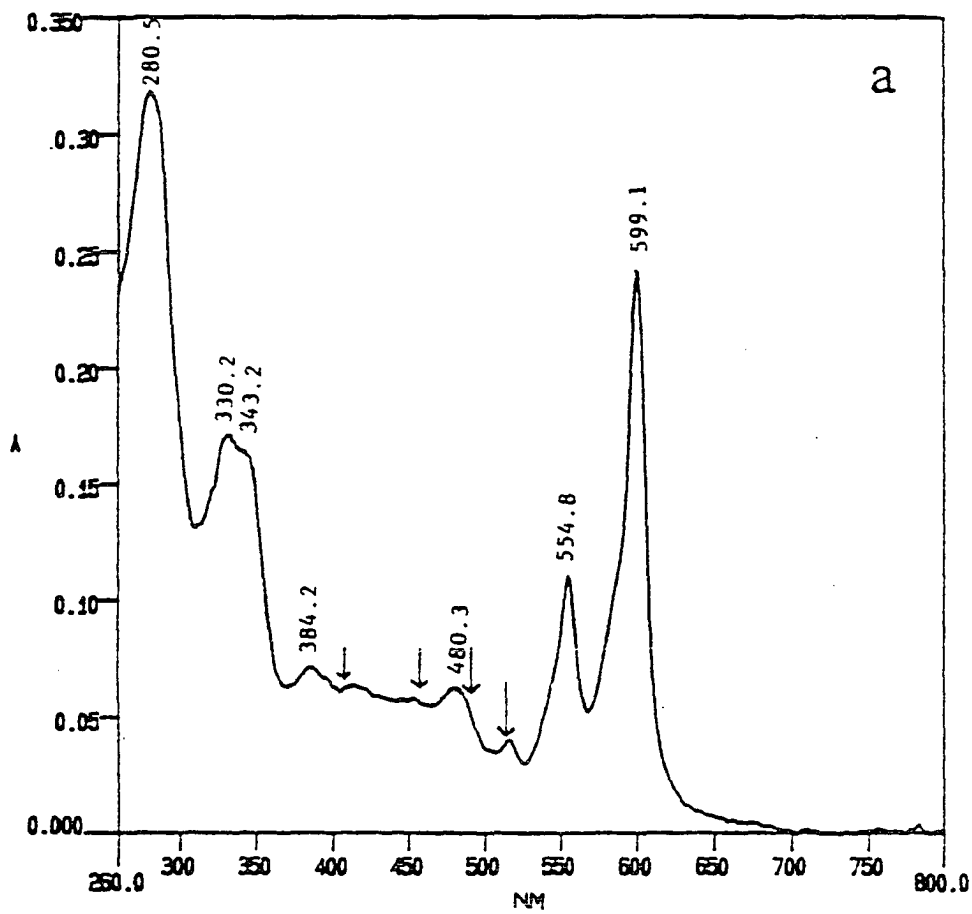

Figure 2. Absorption spectrum of hypericin (10^{-4} M in DMSO)

Meruelo *et al.*[10,11] have examined the efficacy of hypericin with respect to several viruses including HIV; however, no light dependance was reported. Hudson *et al.*[8] and Lopez-Bazzocchi *et al.*[9] both noted the effect of light (absence or presence) on the antiviral effect of hypericin. Illumination was provided by a tungsten lamp with continuous emission between 380 and 700 nm. This work,[8,9] also reported the presence of a dark mechanism which resulted in some viral inactivation although not as much as when light was present. Carpenter *et al.*[7] have reported that EIAV inactivation by hypericin required the presence of light. In direct contrast to earlier studies, no dark mechanism or toxicity were observed at the concentrations (10 μg/ml) used in this work.

Viral inactivation by hypericin at different excitation wavelengths was determined. The greatest amount of inactivation was seen at 350 nm (Figure 3). There was no noticeable inactivation from the control (DMSO) samples. The corrected intensities of the incident radiation at each of the wavelengths is listed in Table 1. The highest incident power was at 700 nm followed by 350, 450, 600, and 500 nm. Unfortunately, to conclude anything from this part of the experiment would be presumptuous. This experiment must be repeated with a light source that has the same output at each of the wavelengths of interest. Additionally, an experiment to determine the number of photons impinging on the sample at each wavelength (actinometry) would also be of use.

Table 1

Excitation wavelength (nm)	Corrected relative intensity (mV)
350	0.959
450	0.567
550	0.438
600	0.450
700	2.06

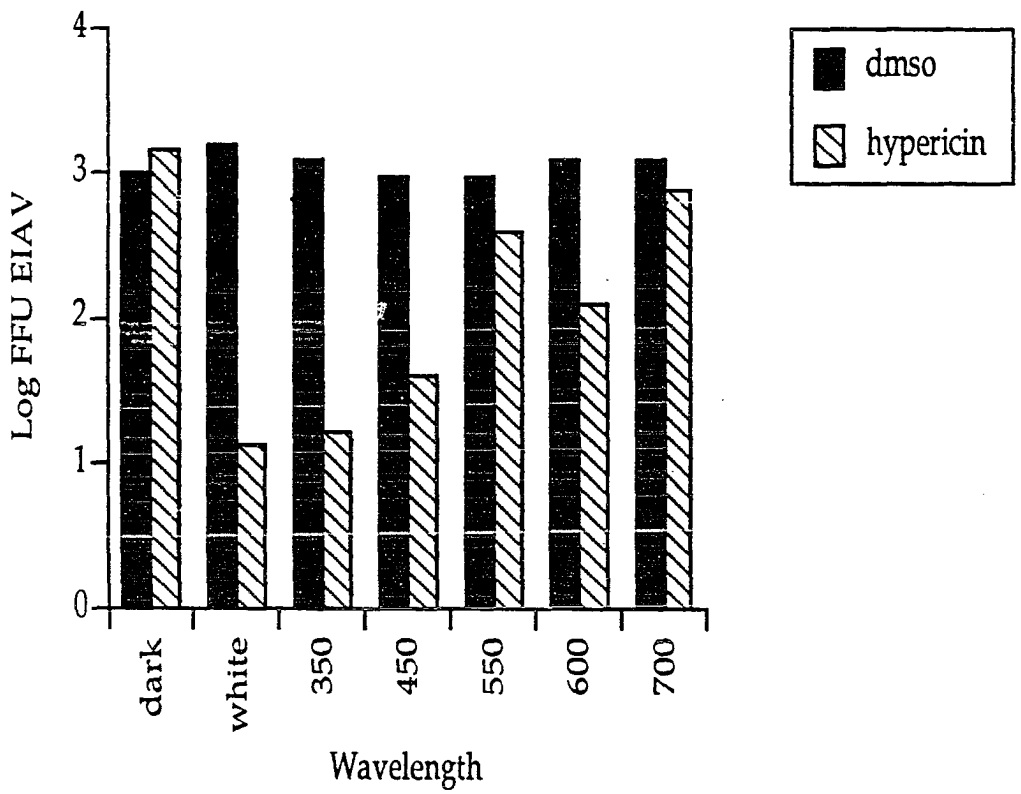

Figure 3. Wavelength dependence for viral inactivation. Control samples contain virus with DMSO

It has been demonstrated that the light intensity is inversely proportional to the length of time needed for photosensitization to occur. In these experiments, 20 minutes was sufficient at the intensities shown in Table 1. It appears that the reason for the large decrease in viral infectivity at 350 nm may be due to the higher power at this wavelength compared to the other wavelengths used. There was no noticeable inactivation at 700 nm which is expected because hypericin does not absorb at this wavelength. Other wavelengths within the ultraviolet region of the spectrum were not tested.

Florescence spectra for the four compounds were obtained. However, the spectra were of poor quality. SERRS proved to be more sensitive than florescence and the spectra for these samples are displayed in Figure 4. The SERRS spectrum of free hypericin (see Raser, *et. al.* [20]) is similar to that seen for MDBK/hypericin and EIAV/hypericin. This indicates that the hypericin is adsorbed near the surface of the virus so as to be enhanced by the silver surface. (The similarities also suggest that the adsorption mechanism is the same for all of the samples.) The intensity of the hypericin bands in the EIAV/hypericin spectrum appear somewhat weaker than the hypericin bands in the MDBK/hypericin spectrum. A lesser intensity would be expected as most of the hypericin from this preparation was not associated with the virus particles and was removed from the sample.

The vibrational bands seen in the SERRS spectra are tentatively assigned to CC in-plane bending modes.[20] However, until further studies with model compounds are completed a more specific

assignment is not warranted. Hypericin has been shown to form strong coherent monolayers either as a pure compound or as a component in phospholipid monolayers. Additional experiments involving model membrane systems are needed to determine the location and environment of hypericin within a membrane. Results from model systems and those involving virus/hypericin complexes may lead to a more exact understanding of the interactions between the hypericin and virus particles.

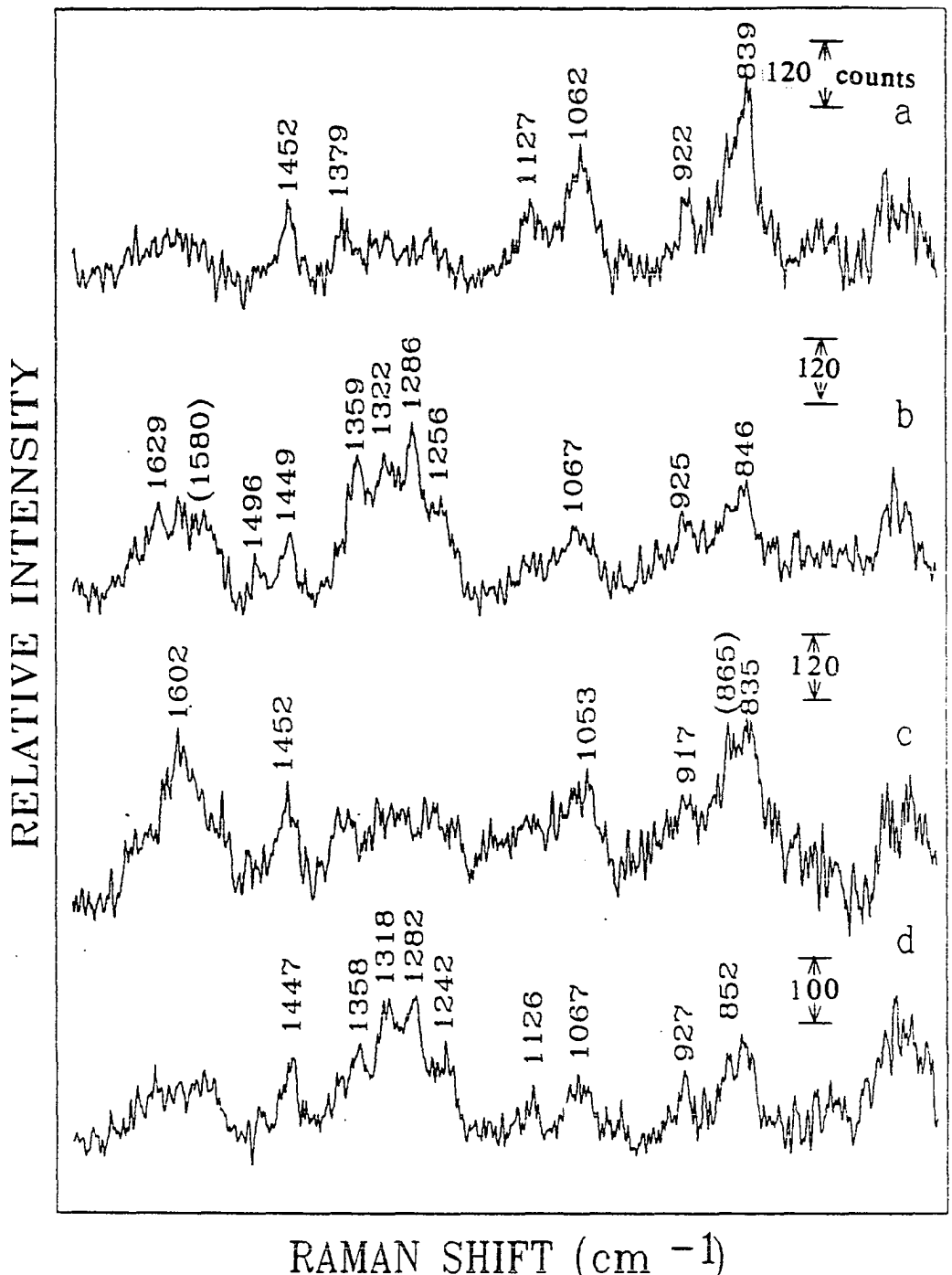

Figure 4. SERRS spectra of a) MBDK, b) MBDK with hypericin, c) WYO (strain of EIAV), and d) WYO with hypericin

CONCLUSIONS

Hypericin, with it photodynamic effect against several viruses and its low toxicity to host cells, may someday become a viable drug for the treatment of viral diseases. The results presented here substantiate the finding that viral inactivation by hypericin requires light. In addition, we have attempted to elucidate the nature of the interaction between hypericin and EIAV. Experiments involving model membrane systems will be used to suggest the location of the hypericin molecules in relation to the virus.

ACKNOWLDEGEMENT

This work was supported by a Biotechnology grant from Iowa State University. Thanks to Yvonne Wannemuehler for her help with the viral inactivation experiments.

REFERENCES

(1) Giese, A. C. In *Photophysiology*; A. C. Giese, Ed.; Academic Press: New York, 1971; Vol. VI; pp 77-124.

(2) Giese, A. C. *Photochem. Photobiol. Rev.* **1980**, *5*, 220-255.

(3) Thomson, R. H. *Naturally Occurring Quinones;* 2nd ed.; Academic Press: New York, 1971, pp 586-597.

(4) Pace, N.; Mackinney, G. *Journal of the American Chemical Society* **1941**, *63*, 2570-2574.

(5) Blum, H. F. *Photodynamic Action and Diseases Caused by Light*; Reinhold Publishing Corp/: New York, 1941.

(6) Duran, N.; Song, P.-S. *Photochemistry and Photobiology* **1986**, *43*, 677-680.

(7) Carpenter, S.; Kraus, G. A. *Photochemistry and Photobiology* **1991**, *53*, 169-174.

(8) Hudson, J. B.; Lopez-Bazzocchi, I.; Towers, G. H. N. *Antiviral Research* **1991**, 101-112.

(9) Lopez-Bazzocchi, I.; Hudson, J. B.; Towers, G. H. N. *Photochem. Photobiol.* **1991**, *54*, 95-98.

(10) Meruelo, D.; Lavie, G.; Lavie, D. *Pro. Nat. Acad. Sci. USA* **1988**, *85*, 5230-5234.

(11) Lavie, G.; Valentine, F.; Levin, B.; Mazur, Y.; Gallo, G.; Lavie, D.; Weiner, D.; Meruelo, D. *Proc. Nat. Acad. Sci. USA* **1989**, *86*, 5963-5967.

(12) Knox, J. P.; Samuels, R. I.; Dodge, A. D. In *Light-Activated Pesticides*; J. R. Heitz and K. R. Downum, Ed.; American Chemical Society: Washington, DC, 1987; pp 265-270.

(13) Foote, C. S. In *Light Activated Pesticides*; J. R. Heitz and K. R. Downum, Ed.; American Chemical Society: Washington, DC, 1987; pp 22-38.

(14) Heitz, J. R. In *Light-Activated Pesticides*; J. Heitz R. and K. R. Downum, Ed.; American Chemical Society: Washington, DC, 1987; pp 1-21.

(15) Knox, J. P.; Dodge, A. D. *Plant, Cell and Environment* **1985**, *8*, 19-25.

(16) Pace, N. *Am. J. of Physiology* **1942**, *136*, 650-656.

(17) Pace, N.; MacKinney, G. *J. Am. Chem. Soc.* **1939**. *63*, 3594-3595.

(18) Scheibe, G.; Schontag, A. *Chem. Ber.* **1942**, *75*, 2019-2026.

(19) Jardon, P.; Gautron, R. *J. Chim. Phys. Phys.-Chim. Biol.* **1989**, *86*, 2173-2190.

(20) Raser, L. N.; Kolaczkowski, S.; Cotton, T. M. submitted to *Photochem.Photobiol.* **1991**.

GENERAL SUMMARY

Resonance Raman and surface enhanced resonance Raman spectroscopies have been shown to be viable techniques for the study in both in vitro and in vivo biological molecules. Both techniques impart high sensitivity and selectivity when used with biomolecules that contain a chromophore. All compounds utilized in the course of this research had detailed absorption spectra in the visible region which made them particularly suited for resonance Raman spectroscopy.

Small but real differences were observed in the RR spectra of the halogenated chlorophylls. Overall, our assignments, based on these compounds, do agree with assignments obtained from normal mode analysis calculations. However, our results also suggest that modes in the region of 1480 - 1550 cm^{-1} should be reanalyzed as some differences were observed. To extend this study, wavelengths other then 406.7 nm should be used to obtain RR spectra as these wavelengths would give information about different electronic states of these molecules. Normal mode calculations on model compounds more closely related to the halogenated compounds would also be useful.

The long range objective of this project was the synthesis of model compounds to study electron transfer processes in photosynthetic models. Although the work was not completed, the halogenated compounds, especially the brominated materials, should make extremely good intermediates in the synthesis of models for photosynthetic electron transfer model complexes.

SERRS proved to be useful for the study of bacteriochlorophyll degradation products. In model membrane systems, photosynthetic pigments will be present at low concentrations and the amounts of degradation products will be minimal. Because of the sensitivity of SERRS, any degradation products formed should be observed. In addition, the selectivity of SERRS spectroscopy allows degradation products to be monitored with little interference from the nondegraded compounds.

Raman spectra of hypericin and analogs were determined at various wavelengths and general assignments were made. SERRS spectra of free hypericin will be compared with spectra of hypericin in model membrane systems. Spatial information may be obtained because of the distance dependance of SERRS. In addition, SERRS spectra of models of the hypericin/virus complexes may help to determine the environment of these biomolecules in relation to the system as a whole.

REFERENCES

(1) Boldt, N. J.; Donohoe, R. J.; Birge, R. R.; Bocian, D. F. *J. Am. Chem. Soc.* **1987**, *109*, 2284-2290.

(2) Andersson, L. A.; Loehr, T. M.; Cotton, T. M.; Simpson, D. J.; Smith, K. M. *Biochim. Biophys. Acta.* **1989**, *974*, 163-179.

(3) Tobias, R. S. *J. Chem. Ed.* **1967**, *44*, 1-8.

(4) Tu, A. T. *Raman Spectroscopy in Biology: Principles and Applications;* Wiley: New York, 1982, pp 3-41.

(5) Cotton, T. M. In *Spectroscopy of Surfaces;* R. J. H. Clark and R. E. Hester, Ed.; John Wiley & Sons: New York, 1988; pp 91-153.

(6) Campion, A. In *Vibrational Spectroscopy of Molecules on Surfaces;* J. T. J. Yates and T. E. Madey, Ed.; Plenum Press: New York, 1987; Vol. I; pp 223-265.

(7) Aroca, R.; Kovac, G. J. In *Vibrational Spectra and Structure;* J. R. Durig, Ed.; Elsevier Science Publishing Co: New York, 1991; pp 55-112.

(8) Gust, D.; Moore, T. A. In *Photoinduced Electron Transfer III;* J. Mattay, Ed.; Springer-Verlag: New York, 1991; pp 103-151.

(9) Tabushi, I.; Sasaki, T. *Tetrahedron Lett.* **1982**, 23, 1913-1916.

(10) Wasielewski, M. R.; Niemczyk, M. P.; Johnson, D. G. In *13th DOE Solar Photochemical Research Conference;* Colorado, 1989; pp 64-68.

(11) Deisenhofer, J.; Epp, O.; Miki, K.; Huber, R.; Michel, H. *Nature* **1985**, *318*, 618-624.

(12) Norris, J. R.; Schiffer, M. *C & E News* **1990**, 22-37.

(13) Robler, S. J.; Breton, J.; Youvan, D. C. *Science* **1990**, *248*, 1402-1405.

(14) Gregory, R. P. F. *Photosynthesis;* Chapman and Hall: New York, 1989.

(15) Seibert, M.; Picorel, R.; Rubin, A. B.; Connolly, J. S. *Plant Physiol.* 1988, *87*, 303-306.

(16) Moënne-Loccoz, P.; Robert, B.; Lutz, M. *Biochem.* 1989, *28*, 3641-3645.

(17) Hansson, Ö.; Wydrzynski, T. *Photosynth. Research* 1990, *23*, 131-162.

(18) Glazer, A. N.; Melis, A. *Ann. Rev. Plant Physiol.* 1987, *38*, 11-45.

(19) Lagoutte, B.; Mathis, P. *Photochem. Photobiol.* 1989, *49*, 833-844.

(20) Pace, N.; Mackinney, G. *Journal of the American Chemical Society* 1941, *63*, 2570-2574.

(21) Giese, A. C. In *Photophysiology*; A. C. Giese, Ed.; Academic Press: New York, 1971; Vol. VI; pp 77-124.

(22) Giese, A. C. *Photochem. Photobiol. Rev.* 1980, *5*, 220-255.

(23) Pace, N. *Am. J. Physiol.* 1942, *136*, 650-656.

(24) Blum, H. F. *Photodynamic Action and Diseases Caused by Light*; Reinhold Publishing Corp/: New York, 1941.

(25) Walker, E. B.; Lee, T. Y.; Song, P.-S. *Biochim. Biophys. Acta* 1979, *587*, 129-144.

(26) Yang, K.-C.; Prusti, R. K.; Walker, E. B.; Song, P.-S.; Watanabe, M.; Furuya, M. *Photochemistry and Photobiology* 1986, *43*, 305-310.

(27) Song, P.-S.; Hader, D.-P.; Poff, K. L. *Photochemistry and Photobiology* 1980, *32*, 781-786.

(28) Duran, N.; Song, P.-S. *Photochemistry and Photobiology* 1986, *43*, 677-680.

(29) Meruelo, D.; Lavie, G.; Lavie, D. *Pro. Nat. Acad. Sci. USA* 1988, *85*, 5230-5234.

(30) Lavie, G.; Valentine, F.; Levin, B.; Mazur, Y.; Gallo, G.; Lavie, D.; Weiner, D.; Meruelo, D. *Proc. Nat. Acad. Sci. USA* **1989**, *86*, 5963-5967.

(31) Carpenter, S.; Kraus, G. A. *Photochemistry and Photobiology* **1991**, *53*, 169-174.

(32) Hudson, J. B.; Lopez-Bazzocchi, I.; Towers, G. H. N. *Antiviral Research* **1991**, 101-112.

(33) Lopez-Bazzocchi, I.; Hudson, J. B.; Towers, G. H. N. *Photochem. Photobiol.* **1991**, *54*, 95-98.

(34) Knox, J. P.; Dodge, A. D. *Plant, Cell and Environment* **1985**, *8*, 19-25.

(35) Knox, J. P.; Samuels, R. I.; Dodge, A. D. In *Light-Activated Pesticides*; J. R. Heitz and K. R. Downum, Ed.; American Chemical Society: Washington, DC, 1987; pp 265-270.

(36) Foote, C. S. In *Light Activated Pesticides*; J. R. Heitz and K. R. Downum, Ed.; American Chemical Society: Washington, DC, 1987; pp 22-38.

(37) Heitz, J. R. In *Light-Activated Pesticides*; J. Heitz R. and K. R. Downum, Ed.; American Chemical Society: Washington, DC, 1987; pp 1-21.

(38) Khan, A. U. In *Light-Activated Pesticides*; J. R. Heitz and K. R. Downum, Ed.; American Chemical Society: Washington, DC, 1987; pp 58-75.

(39) Ito, T. *Photochemistry and Photobiology* **1978**, *28*, 493-508.

(40) Valenzeno, D. R. In *Light Activated Pesticides*; J. R. Heitz and K. R. Downum, Ed.; American Chemical Society: Washington, DC, 1987; pp 39-57.

(41) Mathis, P.; Rutherford, A. W. In *Photosynthesis*; Amesz, J., Ed.; Elsevier: Amsterdam, 1987; pp 63-96.

ACKNOWLEDGEMENT

I would like to take this opportunity to thank all those involved with my graduate career for making it worthwhile. Dr. Cotton: thank you for your support and guidance during the last four years. It was a pleasure to work with you. Joe, Jae-Ho, Lana, and the Randys: I appreciated all your help and patience when showing me the ropes in The Cotton Club. Jeanne: you have been a wonderful friend and I'm glad you joined the group. You have made the past two years so much better by being here. I don't know if I'll ever have as much fun watching two people play as I do watching you and Joe.

Most of all, thank you Jeff for your love and support. I do appreciate the sacrifices (yes, Iowa!) you made so I could finish this degree. To Allen and Sara Shepherd and Vic and Joan Raser, your encouragement and belief in me was deeply appreciated and I thank you for being there when I needed you.